ATR-FTIR Spectroscopy Tools for Medical Diagnosis and Disease Investigation

4

Maria Paraskevaidi, Pierre L. Martin-Hirsch, and Francis L. Martin

Contents

1 Definition of the Topic

Vibrational spectroscopic techniques are increasingly utilized in biomedical research. Attenuated total reflection Fourier-transform infrared (ATR-FTIR) spectroscopy has been applied extensively to investigate various diseases by determining the chemical and molecular differences coming with the disease. Being label-free, nondestructive, and inexpensive, biospectroscopy could potentially make a perfect diagnostic tool in the years to come.

M. Paraskevaidi · F. L. Martin (✉)
School of Pharmacy and Biomedical Sciences, University of Central Lancashire, Preston, UK
e-mail: flmartin@uclan.ac.uk

P. L. Martin-Hirsch
Department of Obstetrics and Gynaecology, Central Lancashire Teaching Hospitals NHS Foundation Trust, Preston, UK

© Springer-Verlag GmbH Germany, part of Springer Nature 2018

C. S. S. R. Kumar (ed.), *Nanotechnology Characterization Tools for Biosensing and Medical Diagnosis*, https://doi.org/10.1007/978-3-662-56333-5_4

2 Overview

Biospectroscopy's ability to investigate and facilitate in different diseases in numerous ways has been pushing the technique toward clinical implementation over the last years. Vibrational spectroscopy could be applicable to many disease states, likely to detect most changes during transition from a normal to a pathological state or during treatment, as well as to provide novel biomarkers related to a disease. Uncertainty in clinical decision-making could thus be significantly reduced. ATR-FTIR sampling mode is preferred in many cases due to the many advantages coming with it, such as ease of sample preparation or reduced light scattering. In this chapter, we will focus on recent advances of ATR-FTIR spectroscopy in the investigation of various pathological conditions. Several review articles and book chapters have been previously written with regard to vibrational spectroscopy and its applications in disease diagnosis. Nevertheless, what is still lacking is a comprehensive report covering the field of disease-related studies that have employed ATR-FTIR spectroscopy as their main analytical approach. The focus of this chapter is, therefore, placed specifically on ATR-FTIR spectroscopy; herein, key research findings are presented after reviewing the recent literature (from 2010 onward). In addition, in an effort to illustrate the breadth and wide-ranging applications of this spectroscopic method, different types of biological materials (tissues, cells, and biofluids) have been investigated instead of focusing on one sample type only.

3 Introduction

Fourier-transform infrared (FTIR) spectroscopy is a well-established technique used to study and give information on the molecular composition of samples. It has been largely used in biomedical studies and has numerous applications including screening of high-risk populations, disease diagnosis, subtype classification, surgical margin determination as well as monitoring of drugs and disease progression/regression. By using a number of different sample types such as cells, tissues, or biofluids, vibrational spectroscopy yields information on their structural components including proteins, lipids, and carbohydrates. The way this analytical method works could be characterized as disadvantageous and advantageous at the same time, depending on the nature of research to be conducted. In particular, vibrational spectroscopy may not be capable of identifying specific molecules when compared to molecular tests, but it allows the investigation of a range of different molecules simultaneously; thus, it provides an overall status of the examined sample and is ideal for complicated diseases such as cancer, diabetes, or neurodegeneration, which are multifactorial, and studying isolated molecules alone might not give a complete answer [1].

Spectrochemical methods generate a signature fingerprint of biological material in the form of spectra. The most commonly used region for biological samples is the mid-IR region (4000–400 cm^{-1}), which includes stretching vibrations such as S–H, O–H, N–H, and C–H (3500–2500 cm^{-1}), and the so-called fingerprint region (1800–900 cm^{-1}), mainly representative of amide I/II (1600–1500 cm^{-1}), lipids

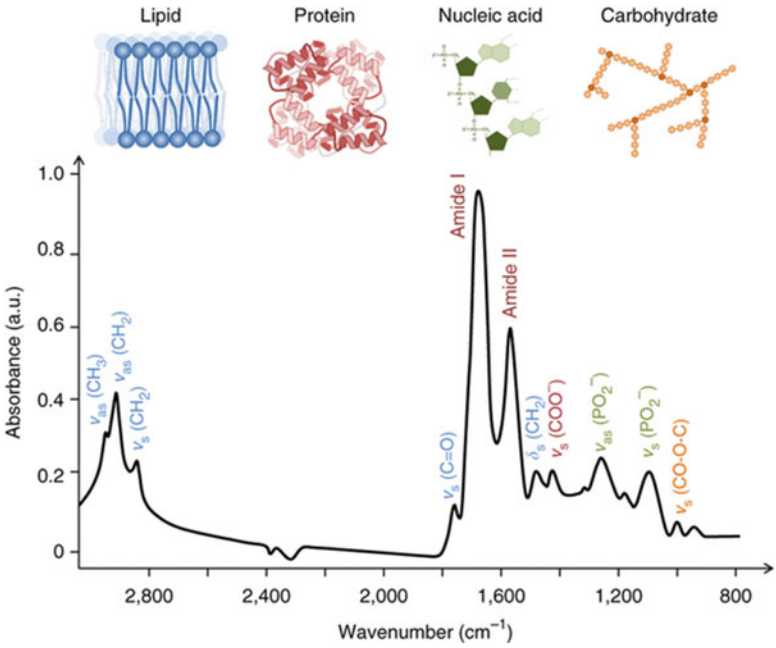

Fig. 4.1 Typical infrared spectrum of a biological sample. ν, stretching vibration; δ, bending vibration; as, asymmetric; s, symmetric. The spectrum was generated in transmission mode from a human breast carcinoma mounted on a CaF_2 slide [4]

(1750 cm^{-1}), carbohydrates (1155 cm^{-1}), asymmetric phosphate stretching vibrations (1225 cm^{-1}), and symmetric phosphate stretching vibrations (1080 cm^{-1}) (Fig. 4.1) [2, 3].

The use of FTIR in attenuated total reflection (ATR) sampling mode is a very promising approach with numerous advantages over transmission or transflection mode, namely, larger sampling area, easier sample preparation, spectral reproducibility, higher signal-to-noise (S/N) ratio, applicability to aqueous samples, and reduced light scattering. ATR-FTIR uses an internal reflection element (IRE) with a high refractive index to direct the beam to the sample; an evanescent wave is created, penetrating the sample a few microns to derive its chemical information. Therefore, the sample has to be in direct contact with the IRE (i.e., ATR crystal) (Fig. 4.2). The angle of the incident IR beam should exceed the critical angle to achieve total internal reflection; otherwise, the resulting spectrum will be a combination of ATR and external refraction (Fig. 4.3).

A number of different diseases have been thoroughly investigated by ATR-FTIR (Fig. 4.4). It would seem that the fastest growing area in vibrational spectroscopy is the diagnosis of various cancers, such as ovarian, endometrial, breast, skin, prostate, brain, colorectal, and others. The advent of IR fiber-optic probes equipped with ATR elements has also allowed for in vivo and in situ diagnostic studies of easily reached organs such as the skin, oral cavity, or colon and gastrointestinal tract through

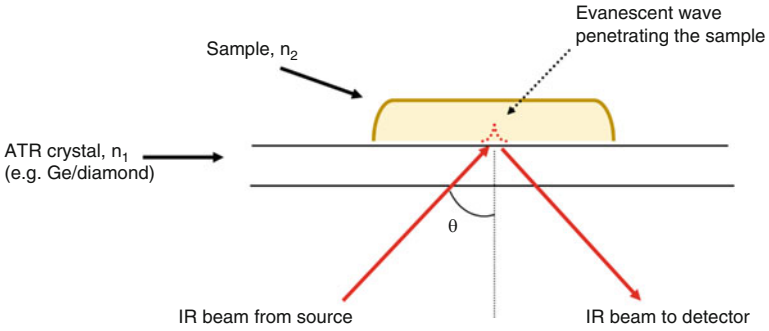

Fig. 4.2 Schematic of the ATR-FTIR sampling mode (n, refractive index; θ, angle of incidence)

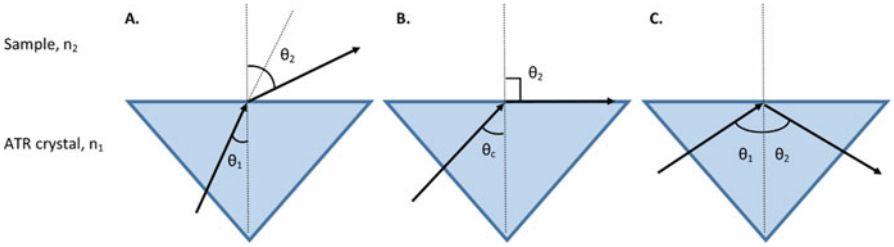

Fig. 4.3 (A) $\theta_1 < \theta_c$, refraction occurs; (B) θ_c, refraction along the boundary; (C) $\theta_1 > \theta_c$, total internal reflection occurs, (θ_c, critical angle)

colonoscopes and endoscopes [5, 6]. However, other pathological conditions have been studied as well, such as rheumatoid arthritis [7], HIV/AIDS [8], alkaptonuria [9], malaria [10], diabetes [11, 12], cystic fibrosis [13], thalassemia [14], kidney diseases [15, 16], prenatal disorders like preterm birth and premature rupture of membranes [17], and neurological diseases like Alzheimer's [18], which are also some examples of the wide-reaching applications of ATR-FTIR spectroscopy.

Suitable sample types for ATR-FTIR spectroscopy include tissues, cells, and biological fluids. Different groups have used endometrial [19], cervical [20], brain [21, 22], ovarian [23], intestine [22], lung [24], skin [25, 26], prostate [27, 28], breast [29, 30], liver [31, 32], colorectal [33], gastric [34], and esophagus [35] tissues – a method known as spectral histopathology (SHP) [36]. Various cell types and populations have also been examined, either fixed or live, derived from epithelial, nervous, muscle, or connective tissue, being either stem cells, transit-amplifying, or differentiated [4, 37–39] – this method is known as spectral cytopathology (SCP) [40]. Some of the biofluids that have been employed for ATR-FTIR analysis are whole blood [41, 42], blood plasma and serum [43–45], urine [9, 42], sputum [46], saliva [47, 48], tears [49], cerebrospinal fluid (CSF) [50], and amniotic fluid [17]. From the above sample types, readily accessible biofluids such as blood, urine, sputum, or saliva are considered ideal for clinical implementation due to the noninvasive, routine methods of collection as well as their minimal sample preparation.

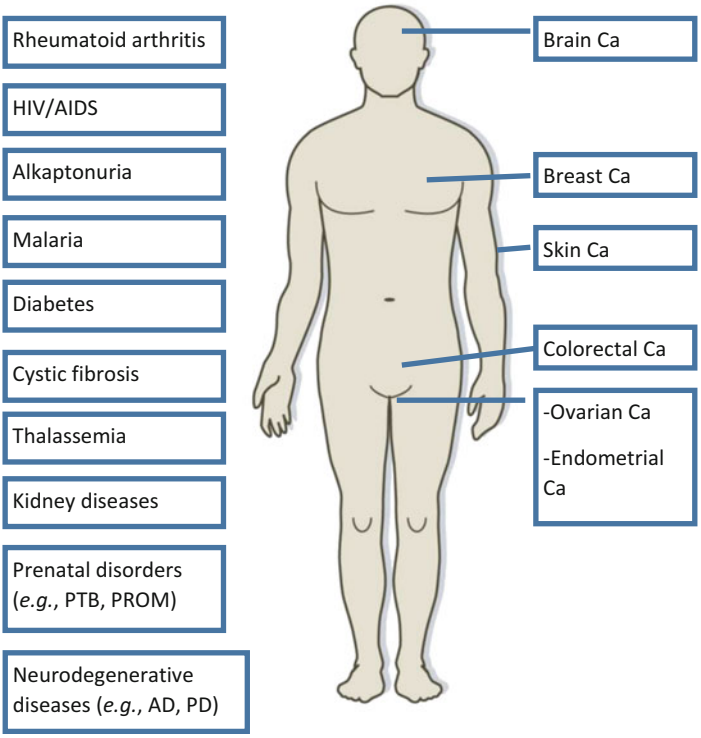

Fig. 4.4 Diseases that have been studied by ATR-FTIR include a number of different pathologies/disorders (HIV, human immunodeficiency virus; AIDS, acquired immune deficiency syndrome; PTB, preterm birth; PROM, premature rupture of membrane; AD, Alzheimer's disease; PD, Parkinson's disease; Ca, cancer)

Early disease detection is of crucial importance as, once the patient appears with clinical symptoms, the condition may already be irreversible. If at-risk individuals are identified early, it may be possible to delay/prevent further progression or provide suitable treatment/medication. As aforementioned, multifactorial diseases may require a panel of biomarkers – defined as disease-associated molecular changes in body tissues and fluids [51] – in order to better comprehend their etiology and facilitate screening and diagnosis, so that appropriate clinical intervention can begin as soon as possible. The necessity of discovering new biomarkers and techniques arises from the lack of highly sensitive and specific biomarkers for a number of diseases, as well as the limited availability of cost-effective and noninvasive tests. For instance, prostate-specific antigen (PSA) levels, used to diagnose prostate cancer in serum, provide sensitivity of ~20% for any stage of the disease and ~50% for high grade [52]; cancer antigen 125 (CA-125) levels, used as a biomarker for ovarian cancer detection in serum, provide sensitivity and specificity of ~80% and 75%, respectively, but are only elevated in half of the individuals at an early stage [53];

estrogen receptor (ECα), used in breast cancer, has varying specificity from 72% to 77% [54]; Alzheimer's disease has been shown to be diagnosed with ~95% sensitivity and ~85% specificity but only after the combination of three different biomarkers in CSF, namely, amyloid-β 42 (Aβ42), total tau, and phospho-tau-181 [55]; serum creatinine, used for screening kidney failure, provides sensitivity of ~13% for any stage and ~45% for severe kidney failure [56].

This chapter will focus on the advancements of ATR-FTIR spectroscopy as a diagnostic tool for the investigation of a variety of diseases; particular focus will be given on experimental and instrumental methodology, as well as potential pitfalls and what to avoid. An in-depth review of all the literature on ATR-FTIR since 2010, along with the key research findings, will also be included. Conclusions, limitations, and an overview of where the field of spectroscopy is heading will be presented.

4 Experimental and Instrumental Methodology

4.1 Experimental Methodology

A variety of different clinical sample types, substrates, preparation, data preprocessing, and multivariate techniques have been employed in the past toward medical diagnosis with ATR-FTIR spectroscopy. It is worth mentioning that even though there is a growing literature proving the diagnostic capability of spectroscopy, there are still many hurdles to overcome for clinical implementation; the most important is the lack of standardization and validation in large clinical trials. A very interesting paper on discovering new biomarkers of disease states that flaws could be introduced in a study even from the very first step of sample collection which could inevitably affect the results of subsequent experiments [51]. For instance, it was recently shown that use of different anticoagulants in blood plasma collection could affect spectroscopic analysis by introducing confounding peaks [57]. Continuous efforts of different groups within the spectroscopy field are made to standardize processes from the pre-analytical phase, such as sample collection/preparation, to the analytical and post-analytical phase, such as optimal spectrometer settings and data handing (Fig. 4.5). In this section, we will discuss some of the most common steps adapted as experimental procedures. The methodology presented here is not exhaustive but rather an overview of the critical steps for ATR-FTIR spectroscopy.

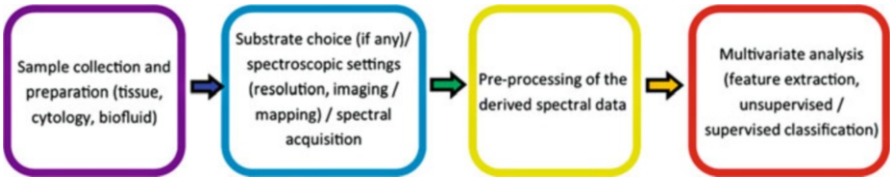

Fig. 4.5 Schematic overview of the steps followed for ATR-FTIR spectroscopy

4.1.1 Sample Collection and Preparation

Tissue: Tissue samples can be either formalin-fixed paraffin-embedded (FFPE) or snap-frozen. For FFPE tissue, the removed biopsy of interest is immersed in an aqueous formaldehyde solution (formalin), which is used as a preservative for biological material. The aim is to remove the water present in tissue and replace it with a medium that solidifies the tissue (i.e., paraffin wax) and allows fine sectioning. Paraffin is immiscible with water; thus, the tissue is first dehydrated with sequential immersions in increasing concentration of ethanol up to 100%, followed by washes in xylene, which is used to remove ethanol. Final step includes embedding of the tissue in molten paraffin wax and cooling down, which hardens the wax. FFPE blocks can be stored at room temperature.

In order for the FFPE tissue to be analyzed with spectroscopy, it needs to be sectioned from the whole tissue block with a microtome, while kept cool onto an ice block to ensure that the wax remains hard, therefore allowing easier sectioning. The tissue ribbons (8–10 μm thick) are put in a warm H_2O bath (40–44 °C) and then floated onto the substrate of choice. The slide with the tissue is then placed in a 60 °C oven for 10 min and de-waxed by immersion in fresh xylene for 5 min, thrice. Finally, immersion in acetone or 100% ethanol follows for 5 min in order to remove the xylene before air-drying in room temperature.

Snap-frozen tissue is preferred for molecular studies as it avoids the use of preservatives and paraffin that cause degradation. For snap-freezing, the tissue is first embedded in optimal cutting temperature (OCT) compound, while isopentane, cooled with liquid N_2, is then used to finally freeze the sample; 60–90 s will be enough for the OCT compound to freeze. Direct immersion of the tissue into liquid N_2 is avoided, as it would destroy cellular morphology and tissue architecture. Each sample can then be wrapped individually in labeled aluminum foil and stored at −80 °C until analysis.

To use snap-frozen tissue for spectroscopic analysis, the frozen block is mounted into a cryostat for 30 min to reach the cryostat's temperature (~ −20 °C). Then, serial sections of tissues (8–10 μm thick) are cut from the block, mounted onto the substrate of choice, and left to dry in desiccant for at least 3 h before analysis. Sections should be carefully collected in order to avoid contamination of the tissue with the OCT. Exposure to light should be minimized until the analysis to prevent tissue degradation due to oxidation.

Cytology: Cells can be either fixed in a preservative solution or live. A well-studied example of fixed cells is cervical cytology; however, the following experimental procedure could be adapted for other cell types kept in fixative buffers. Firstly, the fixative solution (e.g., ThinPrep or SurePath for cervical cells) needs to be removed as it would give unwanted peaks in the fingerprint region; to achieve this, the sample undergoes centrifugation (2000 rpm for 5 min) and the supernatant is discarded. Each sample is resuspended in distilled water and centrifuged again. This washing procedure should be repeated three times. The remaining cell pellet should be finally resuspended in 100 μl of distilled water, deposited onto a substrate of choice with a micropipette, and left to air-dry at room temperature. Another way to apply the cells onto a substrate is by cytospinning; the initial washing steps are

followed as before, and a maximum volume of 200 μl is spun in a cytospin cytocentrifuge so that the cells get squashed onto the slide. Then, they are again left to air-dry and stored in desiccant until their analysis.

Studying live cells rather than fixed ones may be a more challenging technique, but it would allow for in situ measurements and data collection of the same cell at different time points. Cells in suspension should be firstly detached from the growth substrate (e.g., flask) using trypsin and subsequently washed from medium and trypsin with phosphate-buffered saline (PBS). Live cells could then be directly seeded and grown on the ATR crystal with the use of a cell chamber, so that they form a good contact [39]. Another option would be the deposition of a drop of the cell suspension onto a substrate of choice and air-drying at room temperature. An alternative would also be to grow the cells directly onto slides that have been sterilized in 70% ethanol for an hour and rinsed with sterilized water [28]; this would, however, make the cells thin as they grow and stretch over a 2-D surface. Three-dimensional culture matrices (a tissue culture environment or device where live cells can grow in three dimensions) could provide a realistic environment to study cells; after being grown in 3-D cultures, cells should be fixed or snap-frozen as described aforementioned for the tissue samples [4]. Of course, live cells could always be directly fixed in a preservative solution – just as with cervical cytology – and prepared as aforementioned.

Biofluids: The use of biofluids in vibrational spectroscopy has increased rapidly in the last decade, providing a promising and alternative technique to tissue biopsies and cytology. Biofluids already analyzed by ATR-FTIR spectroscopy include some easily accessible, noninvasive samples such as whole blood, plasma, serum, urine, sputum, saliva, and tears as well as some more invasive, organ-specific samples such as cerebrospinal fluid (CSF) and amniotic fluid.

Blood samples are easily collected by venepuncture: whole blood requires no further treatment apart from addition of an anticoagulant [e.g., ethylenediaminetetraacetic acid (EDTA), lithium heparin, or citrate] to prevent clotting; for blood plasma samples, whole blood is collected into anticoagulant-treated tubes and then centrifuged (~1000–2000 rpm for 5–10 min) to remove cells (the resulting supernatant is the plasma); for blood serum samples, whole blood is collected into a tube without anticoagulant, left undisturbed to clot at room temperature for 15–30 min, and then centrifuged (~1000–2000 rpm for 5–10 min) to remove the clot (the resulting supernatant is the serum). Urine samples are collected and typically stored without any sample preparation. Fresh sputum sample can be obtained either by having the patient/individual expectorate into a sterile specimen cup or by following the standard protocol for sputum induction – for those who have difficulty producing sputum spontaneously. If sputum cells were to be studied in isolation, the mucus should be removed before the whole sputum specimen undergoes centrifugation (~3000 rpm for 10 min). Saliva is obtained by expectoration or by use of a cotton swab followed by centrifugation to isolate the saliva; a detailed review specifically dedicated to saliva specimen collection toward disease diagnosis was published a decade ago [58]. Tears

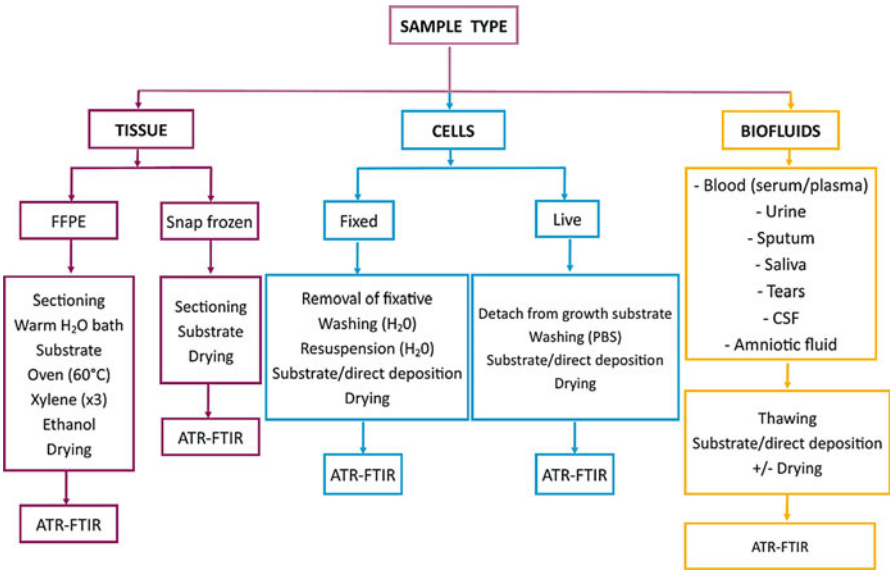

Fig. 4.6 Schematic with the basic preparation steps for different samples toward ATR-FTIR spectroscopy

should be carefully collected without additional stimulation; touching the eyelid and corneal should be avoided in order to avoid reflex tear fluid caused by stimulation. Disposable glass microcapillary tubes and polyester fiber rods have been used for tear collection. The most common collection method for CSF is by lumbar puncture followed by storage with no further sample treatment. Amniotic fluid samples are centrifuged right after collection and their supernatants are subsequently stored.

All of above biofluids are frozen at −80 °C right after their collection, unless they are immediately used. Before spectroscopic interrogation, it is crucial that samples are fully thawed. Generally, the most common method for biofluid deposition before further analysis is by drop deposition and drying either directly onto the ATR crystal or onto an appropriate IR substrate. A schematic summarizing the preparation procedures for all the sample types is shown in Fig. 4.6.

Important considerations: The pre-analytical stages for sample collection and handling can have tremendous effect on the derived spectra and subsequently the interpretation of the result; therefore, standard procedures should be followed carefully. The research community should adapt common standards and interlaboratory data integration for their findings to become clinically useful.

The quality of the samples that are stored at −80 °C could be compromised after a number of freeze-thaw cycles. Freeze-thawing should be avoided when unnecessary or at least be controlled; for instance, biofluids could be divided in aliquots of smaller volume from the initial sample. A recent study has shown the ability of FTIR to

differentiate fresh blood samples from samples that have been freeze-thawed up to five times, but could not distinguish between the five freeze-thaw cycles [57]. However, another study using mass spectrometry has found that freeze-thawing is to blame for changes in the integrity of the samples, especially after two thaws [59].

Fixative solutions, such as formalin for tissue and ThinPrep for cervical cytology, or paraffin wax used for tissue embedding, give characteristic IR spectral signatures and can easily mask biological information of a sample. Paraffin, for example, gives significant peaks at ~2954 cm^{-1}, 2920 cm^{-1}, 2846 cm^{-1}, 1462 cm^{-1}, and 1373 cm^{-1} [4]. Therefore, removal of these sample contaminants and further cleaning of the samples must be thorough. The deparaffinization and cleaning process are not always easy, and subsequent spectral analysis could be employed to exclude the spectral regions that are contaminated. When using biofluids such as blood plasma or serum, careful removal of cells should precede storage if cells are not directly investigated.

Most of the biofluid studies have used dried samples in order to remove the spectral signature of water which dominates the mid-IR region: amide I region (~1650 cm^{-1}) due to water-bending vibration and the higher region (~3000 cm^{-1}) due to –OH stretching vibrations [60]. Drying time of 1 μl of biofluid has been found to be 8 min [61], and typical volumes can range from 1 to 50 μl. However, dried samples can suffer from chemical and physical inhomogeneity which would reduce reproducibility and sensitivity [62]. When a liquid drop is dried on a surface, there is the subsequent appearance of differential crystallization known as the "coffee ring effect" where the majority of the constituents of the sample migrate to the periphery of the drop [63]. This phenomenon leads to inconsistency in the concentration across the sample and should be taken into account before spectral acquisition. Averaging multiple point spectra across the width of the outer ring has been shown to eliminate this issue [64]. Another approach is the analysis of biofluids in their liquid state without or after semidrying, which may "sacrifice" some spectral regions, but it still identifies important bands [65]. Moreover, dried samples often result in higher peaks compared to wet samples, but they have the shortcoming of the uneven distribution [4]; further research of this approach is needed.

Anticoagulants such as citrate, EDTA and lithium heparin are used for the collection of blood plasma to prevent clotting. Citrate and EDTA function by chelating calcium and preventing thiamine-dependent clotting factors from functioning, while lithium heparin binds to antithrombin III clotting factors to prevent their function [66]. Comparing the spectral signature from EDTA and citrate with lithium heparin, the latter was found to give fewer additional peaks and therefore be more appropriate for spectroscopic analysis; after dialysis of the plasma samples with a 10 kDa membrane, the peaks from EDTA seemed to be removed [57]. However, samples collected in the biobanks are used for multicenter studies, and depending on the study, different anticoagulants are preferred. For example, a different group suggested that all of the three anticoagulants are acceptable but EDTA particularly is preferred for delayed blood processing [67]. As long as the use of one anticoagulant remains consistent throughout the dataset, then this issue will be unlikely to have a great effect during spectroscopic comparison.

One of the factors that should be well-considered is the thickness of the sample under interrogation. In the ATR-FTIR sampling mode, the generated evanescent wave, which penetrates beyond the crystal to reach the sample, is ~1–2 μm within the fingerprint region, but 5% intensity still reaches at 3 μm depth. Penetration depth is dependent on the wavelength of the incident light, the refractive indices of the crystal, and the sample, as well as the incidence angle of the IR beam, and is given by the following equation:

$$d_{\mathrm{p}} = \frac{\lambda}{2\,\pi\, n_{\mathrm{IRE}} \sqrt{\sin^2\theta - \left(n_{\mathrm{samp}}/n_{\mathrm{IRE}}\right)^2}}$$

where d_{p} is the penetration depth; λ is the wavelength; n_{IRE} and n_{samp} are the refractive indices of the IRE and sample, respectively; and θ is the angle of incidence. As seen from the above equation, the pathlength is directly proportional to the wavelength so that for longer λ, we get greater penetration; therefore, ATR intensity is decreased for higher wavenumbers. Typical values of d_{p} for a biological sample are ~0.4–0.54 μm for the C–H stretching bands (lipids), 0.75–0.95 μm for amides I and II, and 1.1–1.47 μm for P–O/C–O stretching (nucleic acids and carbohydrates). A commonly used substrate in ATR-FTIR is the IR reflective low-E microscope slide (MirrIR, Kevley Technologies) mainly because of its low cost. This highly reflective slide is essentially a glass slide coated with a multilayer of tin oxide (SnO_2) and silver (Ag). Numerous studies have suggested that, in case of very thin samples, these slides could generate an electric field standing wave (EFSW) effect coming from the metallic surface (Ag), urging careful consideration of the thickness of the samples (>2–3 μm) to avoid potential spectra distortion; therefore, ATR or transmission modes were thought preferable over transflection mode [68]. However, it was also pointed out that by using suitable preprocessing methods (e.g., second derivative), distortions from this phenomenon can be efficiently reduced [40, 69]. Too-thin or too-sparse samples could also lead to low signal-to-noise (S/N) ratio [37]; thus, the samples should ideally be three- or fourfold thicker than the penetration depth, with no maximum thickness limitations. Overall, higher S/N ratio can be achieved when the sample is flat, of adequate thickness, and covers completely the ATR crystal.

4.1.2 Substrates

Substrate choice is an important consideration in IR studies of biological samples due to potential background interference. Substrates used in ATR mode include calcium fluoride (CaF_2) or barium fluoride (BaF_2) slides, MirrIR low-E slides, and zinc selenide (ZnSe) slides; aluminum-coated slides have also shown promise as a substrate in a recent, pilot study – further work with more samples would be needed to validate these results [28]. As aforementioned, caution should be exercised when using low-E slides in micro-ATR experiments to eliminate substrate artifacts generated from very thin samples; instead samples should be >2–3 μm thick. An alternative method, especially for biofluids, could be the direct deposition of a drop on the IRE as it

would avoid any substrate signal contribution. For live cells, a cell chamber can be used to facilitate cells to grow in close contact with the IRE [39].

4.1.3 Spectral Acquisition and Experimental Procedure

Different instrumentation, light sources, and detectors can be used for ATR-FTIR spectroscopy, and each one, along with other variables, could affect the S/N ratio and therefore the quality of the resulting spectra or images. Other parameters affecting the S/N ratio are the sampling aperture, number of co-additions, mirror velocity, and spectral resolution [38]. Once the samples are prepared, as abovementioned, they are deposited either directly on the ATR crystal or on the substrate of choice, and then the spectra can be collected. Generally, intimate contact of the sample with the IRE element is necessary to eliminate background artifacts. Point spectra are typically acquired from multiple locations (ten different locations is common) of each sample to minimize bias. Maps can also be generated by collection of point spectra from an area of interest. The advent of array detectors has also allowed spectral acquisition in imaging mode, which allows for simultaneous collection of spectra. The IRE should be cleaned with a disinfectant solution (e.g., Virkon solution) and distilled water or ethanol and dried every time before moving to the next sample. A background spectrum should be acquired to account for ambient and instrumental conditions. It is recommended to record a background after every sample and at regular intervals to account for atmospheric changes.

4.1.4 Spectral Preprocessing and Multivariate Analysis

Preprocessing of the acquired spectra is an essential step of all spectroscopic experiments and is used to correct problems associated with spectral acquisition, instrumentation, or even sample handling before further multivariate analysis. Depending on the study's goal (i.e., diagnostic, biomarker identification, imaging, or pattern finding), the user has to follow different pathways for the data analysis. A diagnostic approach may be more complex as it requires initial training of the classification system before further validation occurs (e.g., cross-validation).

The main preprocessing methods are de-noising, spectral correction, and normalization. Techniques for de-noising spectra are Savitzky-Golay (SG) smoothing, wavelet de-noising (WDN), and principal component analysis (PCA); the latter is more common and reduces the spectral data space to principal components (PCs) responsible for the majority of variance removing, therefore, the noise. Spectral correction can be applied to spectra with sloped or oscillatory baselines due to scattering, with resonant Mie scattering being the most pronounced effect. Preferred techniques for spectral correction include extended multiplicative scattering correction (EMSC), resonant Mie scattering correction (RMieSC), and rubberband baseline correction. Another way to correct sloped baselines is the use of first or second derivative in combination with SG smoothing; this may alter the shape of the spectra, but it resolves overlapping peaks. Normalization should follow last to account for differences such as varying thickness and concentration that are unrelated to the

biological information; amide I, amide II, and vector normalizations are common. Usually, two or three of the above methods are applied before multivariate analysis; for instance, first or second differentiation is combined with SG smoothing and followed by vector normalization [70].

Subsequently, multivariate approaches are employed to facilitate the handling of the large number of spectral data that is generated. Firstly, feature extraction (FE) is used as a data reduction technique to create new variables based on the original ones; PCA or partial least squares (PSA) are popular as FE methods. Feature selection (FS) can also be used for FE, without altering the original representation of the variables, and can be used to identify the most important wavenumbers that can be used as spectral biomarkers. Further steps include either clustering, which is an unsupervised classification method, with the class of sample being unknown, or supervised classification where the different classes are taken into account. Cluster analysis is an exploratory method and is used for pattern finding and imaging studies; some of the common approaches use k-means, fuzzy c-means, and hierarchical cluster analysis (HCA). Supervised methods estimate the class of an unknown/new dataset after training an initial dataset. Therefore, a training and a validation dataset are required; briefly, some of the supervised approaches are support machines (SVMs), artificial neural networks (ANNs), and k-nearest neighbors (k-NN). If the classifiers lack stability, models can be improved by classifier ensembles as it is accepted that no single model can solve a complex classification problem. We would advise the reader to refer to previous studies that have described the preprocessing and multivariate approaches in more detail as these were beyond the scope of this chapter [4, 38, 70–72].

4.2 Instrumental Methodology

Instrumentation varies for ATR-FTIR studies from benchtop, portable, and handheld instruments to ATR probes. Detectors and internal reflective elements (IRE) can also differ depending on the model of the instrument and the aim of the study. The majority of benchtop spectrometers make use of an inexpensive Globar infrared source. A conventional FTIR spectrometer can provide an enhanced S/N ratio using a synchrotron radiation source as it is 1000 times brighter than the Globar source; however, the combination of micro-ATR with a synchrotron source has not been demonstrated yet [39]. Enhancement of the infrared signal in ATR mode can be achieved with surface-enhanced IR absorption (SEIRA) spectroscopic approaches, according to which molecules on metal surfaces show 10–100 times stronger signal than without the metal [73–76]. This technique is complimentary to surface-enhanced Raman spectroscopy (SERS) and utilizes the surface plasmon effect from the interaction of light with metallic nanoparticles. The principle of this enhanced technique is based on the polarization of the metallic surface (e.g., gold/silver nanoparticles), which generates a local electromagnetic field stronger than the

incident IR photon field; the dipole moment of molecules is, therefore, enlarged, and IR absorption is enhanced.

Spectra can be acquired either as point spectra, which generate maps, or in imaging mode. In mapping mode, chemical information is collected from single/point spectra taken from different locations of a sample, while in imaging, the area of interest is selected and spectra are acquired simultaneously at a specific wavelength to generate pseudo-color images. In conventional ATR-FTIR, a single-element detector is used, meaning that spectra are collected point-by-point having a high S/N ratio; the resulting, high-quality spectrum is indicative of the average signal from the area that the IR light passed. In imaging mode, a large number of spectra are collected simultaneously with the use of array detectors such as linear array and focal plane array (FPA) detectors. Linear array detectors obtain an image by raster scanning of rows of a sample, whereas FPA detectors collect the IR signal from all locations. The use of these detectors in ATR decreases acquisition time by two to three times and achieves high spatial resolutions, down to diffracted-limited resolution values [77]. A fourfold increase of spatial resolution can be achieved in ATR mode, compared to transmission and transflection mode, due to the crystal's (e.g., Ge or Di) high refractive index in the mid-IR [29]. The detector of choice can be either thermal, such as the deuterated L-alanine-doped triglycine sulfate (DLaTGS), or quantum detector such as mercury cadmium telluride (MCT). Despite the latter being better than the standard DLaTGS detector, providing a higher S/N ratio with higher scanning speed and sensitivity, it also needs liquid nitrogen for cooling in contrast to the thermal detector, which operates at room temperatures.

Preliminary experiments should be conducted to find the instrument's optimal conditions before spectral acquisition. These would differ depending on the aim of the study (diagnostic or exploratory) and the preferred spectral and spatial resolution. For instance, the optimal parameters for an ATR-FTIR spectrometer with a diamond crystal of dimensions 250 μm × 250 μm and a single-element detector were found to be 8 cm^{-1} spectral resolution with mirror velocity of 2.2 kHz (1.4 mm/s) and 32 co-additions. It should be noted that resolution should not be higher than necessary, as this would increase total acquisition time significantly. Doubling the resolution, for instance, would require four times higher acquisition time to achieve the same S/N ratio, as S/N ratio of a spectrum is proportional to the square root of the number of co-additions (i.e., acquisition time).

Different accessories and configurations can be used for ATR spectroscopy with the IRE being single or multiple reflection. Single-bounce crystals have smaller sampling areas (~1.5 mm) and are used for strong absorbers and solid samples, whereas multiple-bounce materials have a broad sampling area (~6 mm) providing greater contact with the sample and are used for weaker absorbers or dilutions. Multiple reflection can provide enhanced depth of penetration and sensitivity. ATR crystals include diamond, germanium, zinc selenide, or silicon. The preferred choice for many studies is the diamond crystal due to its robustness and chemical inertness, while other crystals should be handled with caution as they could get scratched or

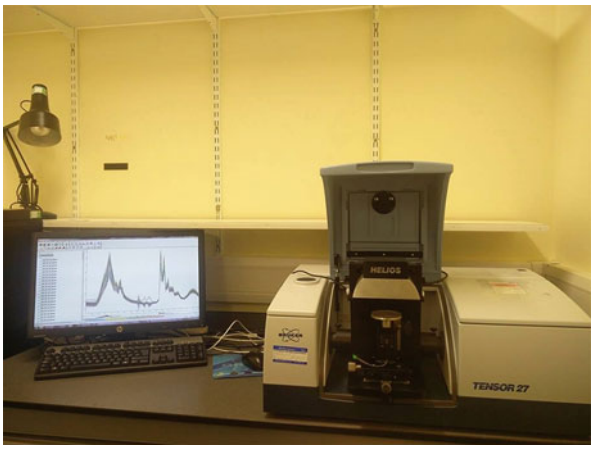

Fig. 4.7 Bruker Tensor 27 FTIR spectrometer equipped with Helios ATR attachment

broken; however, diamond comes at a higher cost. Germanium has the highest refractive index of all ATR materials (~4), which decreases penetration depth (<1 μm) in comparison to the other materials and is useful when highly absorbing molecules are studied. Other spectrometers with ATR attachments (such as the Helios ATR attachment we use for our studies – Fig. 4.7) use a magnification-limited camera to locate the area of interest; however, this configuration cannot provide microscopic features of the sample. ATR probes with IR fiber optics have been also used with various advantages over conventional ATR configurations such as flexibility, low cost, and remote acquirement of spectra (e.g., used for colonoscopes or endoscopes) [78].

A list of various types of instruments used for ATR-FTIR spectroscopy, along with some of their technical characteristics, is shown below:

4.2.1 Manufacturer: ABB Analytical

MB3000 FT-IR analyzer (left): spectral range, 485 to 8500 cm^{-1}; maximum signal-to-noise ratio, 50,000:1; resolution better than 0.7 cm^{-1}; a universal ATR sampling accessory can be used to analyze solids, liquids, pastes, and gels (right); horizontal ATR accessory is also available; solid-state laser; DTGS detector. Photo credit ABB Measurement & Analytics

4.2.2 Manufacturer: Agilent

Cary 630 FTIR Spectrometer: interchangeable sampling accessories for transmission, ATR, specular reflectance, and diffuse reflectance; ATR crystal can be diamond, germanium, or multibounce ZnSe; weights ~4 kg. © Agilent Technologies, Inc. 2011. Reproduced with permission, Courtesy of Agilent Technologies, Inc.

Cary 660 FTIR spectrometer (left): it is only available in conjunction with the Cary 610/620 FTIR microscope systems (right); the Cary 610 is a single-point FTIR

microscope (mapping), while Cary 620 is a focal plane array (FPA) (chemical imaging); the Cary 610 can be upgraded to a Cary 620 providing flexibility depending on the application; ATR accessories are also available. © Agilent Technologies, Inc. 2008. Reproduced with permission, Courtesy of Agilent Technologies, Inc.

4300 Handheld FTIR: a portable system with a variety of sampling interfaces (diffuse reflectance, external reflectance, grazing angle, diamond ATR and Germanium ATR); MCT or DTGS detector; weighs ~2kg. © Agilent Technologies, Inc. 2014. Reproduced with permission, Courtesy of Agilent Technologies, Inc.

4500 Series Portable FTIR: Compact and reliable for non-lab environments; suitable for liquids and solids; the 4500a type uses a spherical Diamond ATR crystal of one, three or five reflections depending on the application; it is ideal for the analysis of solids, liquids, pastes and gels. © Agilent Technologies, Inc. 2011. Reproduced with permission, Courtesy of Agilent Technologies, Inc.

4100 ExoScan Series FTIR (handheld): mid-IR range; suitable for diffuse, grazing angle, specular reflection or spherical ATR sampling interfaces; weighs ~3kg. © Agilent Technologies, Inc. 2011. Reproduced with permission, Courtesy of Agilent Technologies, Inc.

4200 FlexScan Series FTIR (handheld): dual module system, the optical module weighs ~1.5kg and is attached to the ~2kg electronics module by a power cable; it uses the same interferometer and optics as the 4100 ExoScan and thus has identical performance. The ATR interface is ideal for solids, liquids, pastes and gels.

© Agilent Technologies, Inc. 2011. Reproduced with permission, Courtesy of Agilent Technologies, Inc.

5500 Series Compact FTIR: a portable system used for liquid and solid samples; the 5500a type has one, three or five reflection diamond ATRs depending on the application; single reflection diamond ATR available for solids and liquids identification; multi-reflection ZnSe ATR available for liquid analysis. © Agilent Technologies, Inc. 2011. Reproduced with permission, Courtesy of Agilent Technologies, Inc.

4.2.3 Manufacturer: Arcoptix

Arcoptix FTIR-FC (Fiber-Coupling): this system uses ATR fibered probes; it operates in the mid-IR; spectral range, ~5000 to 625 cm^{-1}; there are two options for detectors – MCT, 4-TE cooled, and MCT, liquid N2 cooled; ATR crystal can be

diamond or silicon; probe length, 1.5–1.7 m; ZnSe beamsplitter; solid-state laser at 850 nm; weighs 2.2 kg

4.2.4 Manufacturer: Beijing Beifen-Ruili Analytical Instrument

WQF-510A/520A FTIR Spectrometer: different accessories such as defused/specular reflection, ATR, liquid cell, gas cell, and IR microscope can be attached to the sample compartment; different types of single-reflection ATR crystals can be selected depending on the application (Zn, Se, diamond, germanium, AMTIR, silicon); multiple reflection horizontal ATR (HATR) can also be installed; spectral range, 7800 to 350 cm^{-1}; signal-to-noise ratio, ~15,000:1; DTGS detector; germanium-coated KBr; weighs 28 kg.

WQF-530 FTIR spectrometer: transmission sample holder is standard; optional accessories such as defused/specular reflection, single/multi-reflection ATR, liquid cell, gas cell, and IR microscope can be attached to the sample compartment; spectral range, 7800 to 350 cm^{-1}; signal-to-noise ratio, better than ~20,000:1; resolution, 0.85 cm^{-1}; room temperature DLaTGS detector is used as standard; a temperature stabilized, high sensitivity DLaTGS detector can optionally be used; multilayer Ge-coated KBr; weighs 24 kg.

4.2.5 Manufacturer: Bruker

LUMOS FTIR microscope: 8x objective – magnification can reach 32x by digital zooming; fully automated measurement in transmission, reflection, and ATR mode; in transmission and reflection, the ATR crystal is inserted into the objective; motorized germanium ATR crystal with internal pressure control (three different pressure steps can be software-selected to achieve optimal performance depending on the sample type); large working distance allows samples of ~40 mm thickness; high sensitive photoconductive MCT detector; DTGS detector as option.

HYPERION FTIR microscope: 20× objective; spectral range from visible (up to 25,000 cm^{-1}) to far-IR (down to 80 cm^{-1}); dedicated ATR objective; internal pressure sensor ensures optimal contact between the sample and the crystal; option to connect external accessories.

TENSOR II FTIR spectrometer: large sample compartment to accommodate any FTIR external accessory; fully automated PQ (performance qualification) and OQ (operational qualification) routines for instrument validation; it can be equipped with broadband beamsplitters to expand the spectral range either to the near- or far-IR; room temperature DTGS detector – easily exchangeable; long-life diode laser.

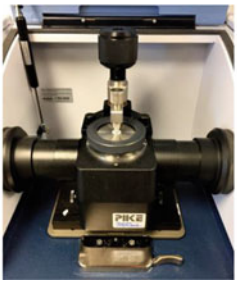

TENSOR 27/37 spectrometers: Tensor 27 is equipped with a Globar source that emits mid-IR light; Tensor 37 has both mid-IR (Globar) and near-IR (tungsten halogen lamp) sources; HeNe laser (emits red light of 633 nm) controls the position of the moving interferometer mirror and is used to determine the sampling positions; DLaTGS detectors are used in both systems with optional, liquid-N2 cooled MCT detectors; different accessories (middle, right) can be attached to the sample compartment area and allow for measurements in the ATR mode.

ALPHA FTIR spectrometers: transmission, ATR, external, and diffuse reflection sampling accessories are available; ALPHA's Platinum ATR (left) uses a single-reflection diamond ATR crystal – it is easy to clean as the pressure applicator can be rotated 360° to provide easier access to the sampling area; Eco-ATR (middle) can be used for powder, solid, paste, and liquid samples – uses a single-reflection, ZnSe ATR crystal; multireflection-ATR module (right) is designed for six internal reflections, is equipped with a horizontal ZnSe ATR crystal, and is suitable for the analysis of pastes, gels, and liquids

4.2.6 Manufacturer: Interspectrum

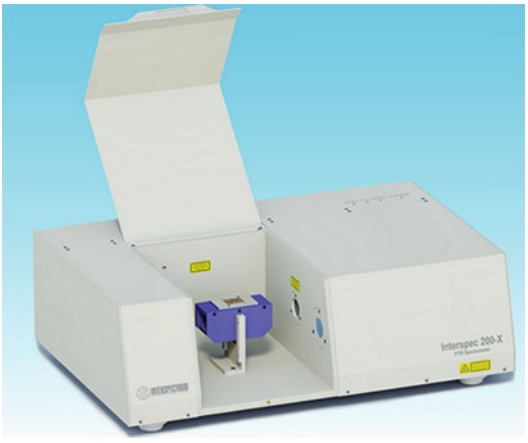

Interspec 200-X: wavelength range in mid-IR: 7000 to 400 cm^{-1}; wavelength range in near-IR: 14,000–5800 or 9000–3850 cm^{-1}; DLaTGS detector (standard) with MCT detector as optional; weighs 24 kg; signal-to-noise, 15,000:1; different accessories are also available for ATR, specular reflection, diffuse reflection, and more.

Interspec 300-X series FTIR spectrometer: portable system; wavelength range, 7000 to 400 cm^{-1}; KBr beamsplitter (standard) – ZnSe beamsplitter (optional); integrated accessories for ATR (horizontal, one bounce with a ZnSe ATR crystal), reflection and transmission measurements; DLaTGS detector; weighs 18 kg; signal-to-noise, 12,000:1.

Interspec 311 Compact FTIR spectrometer: wavelength range, 7000 to 400 cm^{-1} (KBr optics) and 5000–600 cm^{-1} (ZnSe optics); KBr beamsplitter (standard) – ZnSe beamsplitter (optional); weighs 10 kg.

Interspec 650-X Compact FTIR spectrometer: wavelength range, 7000 to 400 cm^{-1} (KBr optics) and 5000–600 cm^{-1} (ZnSe optics); KBr beamsplitter (standard) – ZnSe beamsplitter (optional); weighs 14 kg; different accessories are available or this system, e.g., horizontal one bounce ZnSe ATR accessory (left), three bounce ZnSe ATR accessory (middle), and one bounce ZnSe or diamond ATR accessory.

4.2.7 Manufacturer: JASCO

FT/IR-4000 series FTIR (left): temperature stabilized DLaTGS detector; MCT detector optional; spectral range 5000–220 cm^{-1}; manual or automatic instrument validation; accepts different accessories for the ATR sampling mode such as the ATR PRO ONE (middle) and ATR PRO ONE VIEW (right).

FT/IR-6000 series FTIR: measurements from the near-IR (15,000 cm^{-1}) to the far-IR (50 cm^{-1}); DLaTGS detector with Peltier temperature control

(standard); choice detectors, DLaTGS, MCT, indium antimonide (InSb); manual or automatic instrument validation; accepts different accessories for the ATR sampling mode.

IRT-7000 Series Microscope (left): these systems can be interfaced with the FT/IR-4000 and FT/IR-6000 Series spectrometers (right), offering advanced imaging systems; two detectors as standard, a 16-channel linear array detector for IR imaging and a single-point MCT detector; standard automatic sample stage allows analysis of a large sample area, multi-area ATR mapping, and imaging of a specific area; up to four objectives and automated switching.

IRT-5000 Series Microscope (left): it can be interfaced with the FT/IR-4000 and FT/IR-6000 Series spectrometers (right); used in the mid-IR for materials identification and forensic analysis or in the near-IR and far-IR for more fundamental research; up to two detectors can be installed: mid-band MCT detector

(optional: Peltier cooled DLaTGS); ability for transmission/reflectance or ATR mapping; automatic XYZ sample stage; multiple objectives with automatic switching.

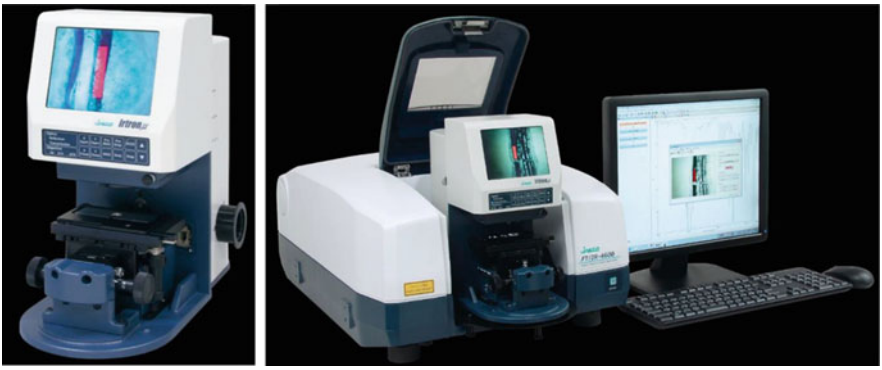

IRT-1000 Series Microscope (left): used with either FT/IR-4000 or FT/IR-6000 Series spectrometers (right); transmittance, reflectance, and ATR modes are available; DLaTGS detector in FTIR main instrument (standard) (MCT or near-IR optimized detector are optional)

4.2.8 Manufacturer: Lumex Instruments

FT-IR Spectrometer InfraLUM FT-08 (left): spectral range, 8000–350 cm^{-1}; signal-to-noise ratio > 4000; DLaTGS detector; weighs 32 kg; different accessories are available such as single (middle) and multiple (right) ATR accessories, diffuse reflectance accessory, and sample compartment microscope; the PIKE MIRacle ATR accessory (middle) is available with five different crystal types [ZnSe, diamond, germanium, silicon, and amorphous material transmitting IR radiation (AMTIR)] and can be used with liquids, solids, pastes, gels, and intractable materials; the horizontal attenuated total reflectance (HATR) accessory (right) is available with the above crystal types and can be used for liquids, semiliquids, solids.

4.2.9 Manufacturer: PerkinElmer

PerkinElmer Frontier: range of near-, mid-, and far-IR Fourier-transform spectrometers; external input and output beam options for custom experiments (left); option for multiple detectors (e.g., DTGS and MCT); different sampling accessories are available; the accessories that can be used for the ATR mode include both multiple reflection HATR and single reflection (right). ©2013–2017 PerkinElmer, Inc. All rights reserved. Reproduced with permission.

Spotlight 150i/200i FT-IR Microscopy System: operates in transmission, reflectance, and automated micro-ATR for maximum sampling flexibility; it can be upgraded to the Spotlight 400 Imaging system (shown below) to allow faster imaging and the opportunity to add ATR imaging. ©2013–2017 PerkinElmer, Inc. All rights reserved. Reproduced with permission.

Spotlight 400 FT-IR Imaging System: automated focus, stage movement, and illumination; contains a single-element MCT detector and a linear array MCT imaging detector; operates in mid-IR, near-IR, or dual range; available sampling modes are standard transmission, reflection, ATR imaging, and more; optional ATR imaging improves spatial resolution. ©2013–2017 PerkinElmer, Inc. All rights reserved. Reproduced with permission.

Spectrum Two IR Spectrometer: portable system; wavelength range, 8300–350 cm^{-1}; weighs 13 kg; DTGS detector is available. ©2013–2017 PerkinElmer, Inc. All rights reserved. Reproduced with permission

4.2.10 Manufacturer: Shimadzu

IRTracer-100 FTIR Spectrophotometer (left): wavelength range, 7800 to 350 cm^{-1} (standard) or 12,500 to 249 cm^{-1} (optional); different accessories (right) can be used for sampling in the ATR mode; single beam; signal-to-noise ratio, 60,000:1.

IRAffinity-1S FTIR Spectrophotometer: wavelength range, 7800 to 350 cm^{-1}; allows measurements in transmission, diffuse reflection, and ATR mode; signal-to-noise ratio, 30,000:1; wide range of accessories are available as above.

4.2.11 Manufacturer: Thermo Fisher Scientific

Nicolet iS50 FT-IR Spectrometer: spectral range from far-IR to visible (15–27,000 cm^{-1}); dual source capable; ATR, Raman, and NIR modules can be used without manually changing system components; three detectors for the main sample compartment; mid-IR and far-IR diamond ATR crystal. Reproduced with permission, Courtesy of Thermo Fisher Scientific.

Nicolet iN5 FTIR microscope: detector options are medium-band MCT-A or room temperature DTGS; 10x objective, N.A. 0.71; transmission, reflection, and optional ATR modes are available; ATR options include pre-aligned, slide-on germanium or diamond crystals; integrated pressure sensor; weighs 29 kg. Reproduced with permission, Courtesy of Thermo Fisher Scientific.

Nicolet iN10 Infrared Microscope: room temperature, deuterated L-alanine-doped triglycine sulfate (DLaTGS) detector (can be replaced by a MCT detector); computer-controlled automation; configurable options: direct contact sampling with MicroTip ATR; manual or motorized stage. Reproduced with permission, Courtesy of Thermo Fisher Scientific.

Nicolet iN10 MX Infrared Imaging Microscope: provides chemical images to enhance understanding of the chemical distribution of heterogeneous samples; DTGS detector (standard); liquid-N2 cooled MCT-A and MCT-A linear array (optional); configurable options, direct contact sampling with MicroTip ATR; best

viewing comfort with dual monitor operation. Reproduced with permission, Courtesy of Thermo Fisher Scientific.

Nicolet iS 10 FT-IR Spectrometer: spectral range 7800–350 cm^{-1} optimized, mid-IR KBr/Ge beamsplitter; 11,000–375 cm^{-1} XT-KBr/Ge extended range mid-infrared (optional); HeNe laser; deuterated triglycine sulfate (DTGS) (standard) detector; liquid-nitrogen-cooled mercury cadmium telluride (MCT) detector (optional); weighs 33 kg. Reproduced with permission, Courtesy of Thermo Fisher Scientific.

Nicolet iS 5 FT-IR Spectrometer: KBr/Ge mid-IR beamsplitter; thermally controlled diode laser; user-replaceable, source, desiccant, power supply, sample compartment windows; deuterated triglycine sulfate (DTGS) (standard) detector; weighs 10 kg. Reproduced with permission, Courtesy of Thermo Fisher Scientific.

Nicolet iS 5N FT-IR Spectrometer: near-IR diode laser; spectral range 11,000–3800 cm^{-1}; CaF2 near-IR beamsplitter; different accessories are included for transmission and ATR modes; iD5 and iD7 ATR accessories offer diamond crystal options; iD5 ATR offers a laminate-diamond crystal, plus heated and multi-bounce crystal plates for special applications; iD7 ATR has a monolithic diamond crystal for the widest spectral range and best durability; interchangeable crystal plates offer good sampling versatility; weighs 10 kg. Reproduced with permission, Courtesy of Thermo Fisher Scientific.

Nicolet Continuum Infrared Microscope: narrow-, mid-, and wide-band MCT-A detector; sampling flexibility with transmission, reflectance, and micro-ATR; chemical image analysis is possible. Reproduced with permission, Courtesy of Thermo Fisher Scientific.

5 Key Research Findings

ATR-FTIR spectroscopy is a powerful technique for the study of various biological specimens and diseases. For spectroscopy to be of diagnostic importance, it is necessary that robust biomarkers exist. For instance, a potential biomarker for cervical cancer diagnosis could be the ratio of glycogen-to-phosphate regions in cells, where increased phosphate levels and decreased glycogen levels would suggest rapid cell proliferation, in turn suggesting malignancy [79]. Apart from its use in disease diagnostics, it also extends to other fields such as screening of high-risk population to identify cells committed to develop disease, classification of different disease subtypes and severity (i.e., low-grade versus high-grade disease), determination of surgical margins, investigation of the effects of a treatment or drug, monitoring of the progression or regression of a disease, and characterization of nanomaterials. With regard to the latter specifically, ATR-FTIR has been utilized for surface characterization of nanomaterials used in biomedical applications. For instance, it has been used to identify chemical features on a surface after its modification to obtain nanosurface features; a respective study by Abbasi et al. revealed a characteristic peak at 1715 cm^{-1}, confirming the modification, and further showed that platelet adhesion was greatly reduced on the modified surface compared to the control, thus providing better blood compatibility [80]. Nanoparticles can be used to introduce drugs into specific sites due to their good uptake within cells. Therefore, Tsai et al. used ATR-FTIR spectroscopy to conduct quantitative analysis of competitive molecular adsorption on gold nanoparticles [81]. A recent study on cell sheet engineering used ATR-FTIR to successfully investigate solvent effect (optimal solvent type and ratio) on nanometric grafting of poly-N-isopropylacrylamide on the surface of polystyrene [82]. Another study explored surface modification of medical polymers which could improve biocompatibility; utilizing ATR-FTIR, normal and modified polystyrene samples (treated with plasma irradiation – oxygen and argon gases) were compared, revealing a significant difference at 3400–3700 cm^{-1} which indicated the presence of functional groups [83]. ATR-FTIR spectroscopy has been used, along with other analytical techniques, to confirm the composition of particles designed as dry-powder inhalation aerosols for targeted respiratory nanomedicine [84]. Investigation of nanoparticle surface composition is crucial in nanotoxicology, but analytical methods to probe nanoparticle surfaces in aqueous are still limited; Mudunkotuwa et al. used ATR-FTIR to study the liquid-solid interface in environmentally and biologically relevant media typically used for toxicity studies [85]. The abovementioned applications have been extremely interesting and advantageous to the scientific community and development of nanomedicine. Some examples of these are briefly reported here; however, the focus of this chapter is on studies using biological samples such as tissues, cells, and biofluids, toward investigation of various diseases.

Currently, most spectroscopic studies are proof of principle, with a small number of cases, showing the potential of the technique in the aforementioned areas; there are only a few large studies using ATR to reach ~500 subjects. In terms of sample size planning, it has been shown that 75–100 samples are required for a good but still not perfect classifier. In the case of smaller datasets, cross-validation is most appropriate as it allows for more robust results after use of different training and validation datasets for a defined number of times [86]. Herein, all of these matters and findings are discussed at more length.

5.1 Tissue

Using an ATR probe equipped with a ZnSe material, oral tissues were examined toward differentiation of malignant from healthy sites. The tumor types examined included adenoid cystic carcinoma, adenoma carcinoma, mulaepidermoid carcinoma, squamous cell carcinoma, basal cell adenocarcinoma, myoepithelioma, and pleomorphic adenoma. It was determined that normal tissue had stronger lipid (~1745 cm^{-1}) and amide I bands in contrast to malignant tissue which also had strong O–H stretching bands [5].

Via ATR-FTIR spectroscopy, Taylor et al. [19] examined endometrial tissue, from tumor and tumor-adjacent tissue, to discriminate benign from malignant areas. The spectral regions that showed significant differences were the lipid and amide I and II (indicative of secondary protein structure) regions. An accurate diagnosis based on spectroscopy would allow for an objective interpretation, eliminating the possibility of human error during microscopic histological examination.

In a preliminary study of 30 patients with lung tumor, ATR-FTIR was employed to discriminate malignant from nonmalignant lung tissue [24]. Sixty lung tissue samples (30 malignant and 30 nonmalignant) were obtained in total from 30 patients. After histological examination, it was verified that 96.7% of original grouped cases was correctly classified. The spectral bands that were mostly responsible for segregation between the two classes were related to proteins at amides I, II, and III, carbohydrates (~1120 cm^{-1}), and nucleic acids (~1085 cm^{-1}).

A recent paper by Theophilou et al. [27] revealed differences in prostate tissue collected from individuals at different time points during a 30-year period, 1983–2013. The changes were mostly attributed to DNA/RNA suggesting that phenotype of the human prostate was altered due to genotoxicity or epigenetic changes; this was also confirmed by immunohistochemical studies for DNA methylation.

Ovarian tissue has been studied with ATR-FTIR spectroscopy to reveal differences not only between benign, borderline, and cancerous tissue but also between the different carcinoma subtypes such as carcinosarcoma and clear cell [23]. Differential diagnosis of the various subtypes/grades would allow an appropriate treatment method such as surgery alone or adjuvant chemotherapy and close follow-up. Classification rates were further optimized when the different subtypes were compared in pairs.

The potential of ATR-FTIR has also been proven in the diagnosis of brain tumors using tissue sections. Gajjar et al. [21] achieved differentiation of various tumor subtypes from healthy tissue. Different ratios of important peaks were also calculated which could be utilized as potential biomarkers. For instance, decreased lipid-to-protein ratio (1740 cm^{-1} to 1400 cm^{-1}) was linked to increased tumor progression, while RNA-to-DNA ratio (1121 cm^{-1} to 1020 cm^{-1}) was reduced in meningioma and metastatic tumors when compared to normal brain tissue.

In a different study, rat tissues were analyzed by ATR-FTIR to explore their biochemical differences and composition [22]. The observed changes were consistent with the expected composition of each tissue: the brain, lung, heart, liver, intestine, and kidney. This finding could be used in pharmacological/pharmacokinetic studies to correlate the biochemical status of the sample with the changes that have occurred. For instance, this could potentially be used to follow up individuals or to monitor the effects of a specific drug to a specific tissue/organ.

Another pilot study using ATR-FTIR has shown its potential to evaluate surgical resection margin in patients with colorectal cancer. Spectra were acquired from tissue obtained from four parts: tumor sample and intestinal mucosa samples from 1 cm, 2 cm, and 5 cm away from the tumor. Spectroscopic analysis showed that spectra from the tumor area and mucosa 1 cm away from tumor were substantially different from those further away from tumor. The differences included decrease of the lipid region and increase of the protein and nucleic acid regions at the tumor and its closest site [33].

Relatively recently, ATR-FTIR spectroscopy was also used intraoperatively in fresh tissue to distinguish benign from malignant breast tissue [30]. Right after spectroscopy, the removed breast tissues were formalin-fixed and sent for histopathological examination; 50 cases were diagnosed as fibroadenoma and 50 cases as invasive ductal carcinoma. The spectroscopic results after classification showed excellent agreement with histological results, with sensitivity and specificity of 90% and 98%, respectively. These findings highlight spectroscopy as a useful investigative tool that could facilitate surgical decisions during an operation and be an alternative to pathological diagnosis of frozen or formalin-fixed tissue sections.

Biochemical changes were also monitored in normal skin tissue of mice after inducing squamous cell carcinoma (SCC) by multistage chemical carcinogenesis. SCC is a nonmelanoma skin cancer and the second most common type of skin cancer. Absorption intensities and band shifts in the peak position were altered in the neoplastic tissue, indicating changes in the secondary structural conformation of proteins. The obtained classification accuracy was 86.4% with sensitivity and specificity of 97.1% and 75.7%, respectively [26]. The authors conclude on the potential of ATR spectroscopy to facilitate diagnosis of SCC.

ATR-FTIR spectroscopy has recently been applied to understand therapeutic responses of cancer patients [87]. There is an increasing need to predict the outcome of a treatment given to cancer patients, but currently, the conventional methods include laborious, time-consuming, and subjective methods. Kalmodia et al. utilized tissue from the mouse xenograft model of retinoblastoma and nanoparticle-mediated targeted therapy (with gold nanoparticles) and showed unique spectral signatures

between treated and untreated subjects, indicating different underlying mechanisms. The results propose that ATR-FTIR could be used to monitor patients' response to cancer therapeutics.

Recent focus in spectrochemical methods has been given to the development of a cost-effective and robust substrate that would allow implementation into a clinical environment. Cui et al. have therefore employed aluminum foil as an alternative substrate, showing that it is able to perform equally or even better than the expensive, conventional substrates. Promising results in an amphibian cell and prostate tissue indicated that this readily available substrate could be used to prepare cytology and histology samples for spectroscopic interrogation without any substrate interference [28]. Undoubtedly, more research is required to achieve final and wider implementation.

5.2 Cytology

Sputum cells have been used by Lewis et al. in an attempt to develop a diagnostic tool for lung cancer [46]. Sputa from 25 lung cancer patients and 25 healthy controls were collected for this observational study; the bronchial origin of the samples was confirmed by the presence of bronchial epithelial cells in H&E-stained cells. The two classes were clearly separated after multivariate analysis with discriminating wavenumbers assigned to protein, nucleic acid, and glycogen changes and seen at 964 cm^{-1}, 1024 cm^{-1}, 1411 cm^{-1}, 1577 cm^{-1}, and 1656 cm^{-1}.

Using cervical cytology, Kelly et al. [88] used two different datasets to train and validate their classification algorithm (dataset A, samples designated as normal, low-grade, and high-grade; dataset B, low-grade samples). The authors concluded that ATR-FTIR spectroscopy could be used to correctly classify the low-grade samples (i.e., dataset B) and maybe subdivide them according to their biological progression or regression "signature." By comparing the ratio of normal/low-grade/high-grade classification per patient, this would allow earlier prediction of the progression or regression before distinct cellular changes were observable by a cytologist. For example, a patient was predicted as 42% normal/47% low-grade/11% high-grade and was negative for the human papillomavirus (HPV) which is associated with the development of cervical cancer. In case of high-grade prediction, further examination would be required as it is linked with more chances for progression.

ATR-FTIR imaging provides the highest spatial resolution, compared to transmission and transflection mode, due to the high refractive index of the IRE in the mid-IR. Walsh et al. [29] applied ATR-FTIR imaging to identify and acquire high-quality chemical information of cell types such as endothelial cells, myoepithelial cells, and terminal ductal lobular units (TDLUs) as well as structure in human breast tissues such as normal, hyperplastic, dysplastic, and malignant tissues. Changes in the structure of DNA during breast cancer were also investigated in extracted intact chromosomes from MCF-7 breast cancer cells. Results of this study pointed out

spectroscopy's ability to resolve and examine a sample at a subcellular level for a more detailed insight of a disease.

A study by Lane and Seo utilized ATR-FTIR to find the structural differences between cancerous breast cells (MCF-7 line) and normal breast cells (MCF-12G line) that contained gold nanoparticles [89]. Different concentrations of nanoparticles were applied in order to study the enhancement of the IR signal (similar to SEIRAS approach – see Instrumental Methodology). They found the nanoparticles within the cells and concluded that increased concentration resulted in sharper peaks and thus easier identification of the differences between the two groups. Findings of this specific study suggest that ATR-FTIR in combination with gold nanotechnology could be used toward cancer diagnosis.

Beta-thalassemia major (β-TM) is caused by a genetic defect in hemoglobin synthesis and results in ineffective erythropoiesis; it is also another disease that has been studied by ATR-FTIR. For the purpose of this study, bone marrow mesenchymal stem cells (BM-MSCs) were collected to investigate global structural and compositional changes in β-TM. Increased lipid, protein, glycogen, and nucleic acid levels were seen in thalassemic patients in contrast to healthy individuals, which were attributed to enhanced cell proliferation and bone marrow activity during ineffective erythropoiesis. Moreover, comparison of the BM-MSCs before and after transplant showed a significant decrease in the content of the aforementioned molecules showing the effect of the transplantation. The observed changes were confirmed by further molecular tests, such as ELISA [14].

Laboratory infected red blood cells (RBCs) have been analyzed with ATR for the detection and quantification of early-stage malaria parasite infections [10]. Early stages of the malaria parasite's life cycle were distinguished, namely, the ring and gametocyte forms, which are the only stages present in peripheral blood, with an absolute detection limit of 0.00001% parasitemia (<1 parasite / μl of blood) and quantification limit of 0.001% (10 parasites per μl). After preliminary studies to select the optimum fixative, methanol was the solution of choice among ethanol and formaldehyde solutions; the samples were then deposited and dried on the crystal. A second study from the same group used infected RBCs in their aqueous state and reported less effect of the anticoagulants compared to the dried state. The authors suggested that the effect was less pronounced presumably because the water diluted the amount of anticoagulant [66]. A large cohort clinical trial led by Wood et al. is ongoing, using portable ATR-FTIR spectrometers toward early diagnosis of asymptomatic carriers of malaria in remote, developing countries.

Another study has employed micro-ATR-FTIR imaging of fixed fibroblast cells to identify the region of the cells where spectral changes occurred upon cancer activation [90]. Predominant changes were attributed to nucleic acids and the C–H stretching of proteins and were mostly seen in the cells' cytoplasm rather than the nucleus, showing that the cells were undergoing a phenotypic change denoted by protein modification.

A more recent, large-scale study using liquid-based cytology (LBC) was conducted toward segregation of the different grades of cervical dysplasia, i.e., normal, low-grade, and high-grade. Even though a degree of crossover between

the classes was seen, attributed to the imperfect conventional screening (i.e., visual examination under the microscope), significant spectral differences were still noticeable [91]. Maximal crossover was found between normal and low-grade specimens, while the least crossover was between high-grade and normal cases, as expected.

A following study utilizing cervical cytology [37] found that ATR-FTIR spectroscopy identified more accurately the underlying disease than conventional screening. This was subsequently confirmed by histology as a "gold standard" approach; histological results were available for almost half of the cases (154 out of 322). When cytology results were used for classification, there was significant overlap between the different categories, whereas when histology results were used, the score plot showed substantially higher segregation between classes.

Using MCF-7 cells, Wu et al. [92] applied different concentrations of a chemotherapy drug (5-fluorouracil) to assess their response. With increasing drug concentration, the band at 1741 cm^{-1}, representative of membrane phospholipids, was increased and an upward shift from 1153 cm^{-1} to 1170 cm^{-1} was noted. The ratio of lipid/amide I (i.e., 1741 cm^{-1}/1640 cm^{-1}) was correlated with the percentage of apoptotic cells. The results indicate that 5-fluorouracil alters the phospholipid composition of the cell membrane, which increases permeability and fluidity, and could be utilized to drug monitoring and improvement of treatment strategies.

The impact of local treatment for precancerous lesions of the cervix has also been investigated with ATR-FTIR in cervical cells [93]. Samples were collected from before and after the treatment (6 months), and significant increase of amide I/II was shown in the posttreatment group, which was attributed to increased cellular function during wound healing from the treatment. Moreover, decreased levels of lipids in the posttreatment indicated the higher bioavailability in the population before treatment. Results from Halliwell et al. showed that excisional treatment, rather the removal of the disease, should be blamed for alterations of the biochemistry of the cervix, which is associated with the higher risk of preterm birth, evident in this population.

Detection of cell activation after treatment with an antibody [anti-CD3 (cluster of differentiation 3)] was also feasible in ATR-FTIR mode [94]. Specifically, cell activation of Jurkat T cells was detected within 75 min after the cells encountered the specific immunoglobulin molecules showing that the technique is sensitive enough to measure molecular events. Similarly, it demonstrates its use in monitoring cellular events and responses to particular agents or drugs at different time points after exposure.

A promising application of ATR-FTIR would be the spectroscopic imaging of live cells, which could facilitate in a range of biomedical purposes. Even though live cells are more of a challenge to study that fixed cytology, Andrew Chan and Kazarian [39] recently reported the advantages and developments of ATR imaging in live cells. That said, improvements in spatial resolution of the acquired images would allow for investigation of micron-sized samples and their subcellular features. A novel approach implemented by the same group has introduced optical apertures directly on the ATR objective of an infrared microscope; this allows the angle of light incidence to be controlled, modifying thus the penetration depth. As a result,

someone would be possible to derive spectral information from different thicknesses of the same sample, as well as to reduce the effects of anomalous dispersions by modifying the angle of incidence.

5.3 Biofluids

Using blood plasma and serum in a pilot study, Gajjar et al. [44] employed ATR-FTIR to diagnose endometrial and ovarian cancers. Using a classification machine, the authors were able to detect ovarian and endometrial with accuracy ~97% and ~82%, respectively. The less promising results in endometrial cancer were attributed to the fact that it is less aggressive than ovarian cancer and most of the times diagnosed in early stages when it is still confined to the uterus. Plasma was also shown to provide higher classification results than serum, which was attributed to the higher number of molecules present in this type of biofluid.

Detection of drugs was suggested in easily acquired saliva samples. Hans et al. [48] used cocaine as a commonly used drug and were able to identify it at a concentration of 0.020 mg/ml. Alcohol's spectral signature was also taken into account as it is common for drugs to get consumed alongside with alcohol. The authors showed a distinct, time-dependent decrease of the alcohol peak (i.e., sugars at ~1050 cm^{-1}) between the time point right after alcohol consumption and 2 h later. Therefore, alcohol was not considered to affect the important spectral region for cocaine detection (1800–1710 cm^{-1}). No preparation or extraction procedures were used for the saliva samples apart from the drying of the sample to eliminate the strong water absorption.

Khanmohammadi et al. were able to discriminate blood serum samples between 35 patients with renal failure and 40 healthy individuals with 95.12% accuracy [15]. The samples were analyzed without any further preparation such as drying or pre-concentration. To eliminate water interference, a background of water was first obtained which was then subtracted from the resulting spectra.

Prenatal disorders such as fetal malformations, preterm birth, and premature rupture of membranes have been investigated toward the development of an early prenatal diagnostic tool. Graça et al. [17] used amniotic fluid from second trimester pregnant women and divided them, according to their pregnancy outcomes, into healthy term pregnancies or the abovementioned disorders. The study demonstrated the ability of ATR-FTIR to accurately diagnose fetal malformations and preterm birth, while for cases or premature rupture of membranes, only minor changes were observed. The authors concluded that using predictive models and a larger cohort, it might be possible for future studies to simultaneously differentiate healthy pregnancies from potential disorders.

HIV/AIDS has been studied by ATR-FTIR in blood serum. The cohort consisted of 39 HIV-affected patients who were on antiretroviral treatment, 16 HIV-affected patients with no retroviral treatment, and 30 uninfected individuals. Both HIV-infected groups were segregated from the healthy individuals with significant differences at lipids/fatty acids (3010 cm^{-1}), carbohydrates (1299 cm^{-1};

1498 cm^{-1}), glucose (1035 cm^{-1}), and proteins (1600 cm^{-1}; 1652 cm^{-1}). Apart from the differential diagnosis of the aforementioned groups with <90% accuracy, the derived spectral biomarkers could be utilized as indicators of response to treatment and/or disease progression. The spectral data were also relatable to more sensitive metabolomic techniques such as nuclear magnetic resonance (NMR) spectroscopy and mass spectrometry (MS), which had been employed before ATR-FTIR from the same group [8].

Serum data by Hands et al. [95] showed differentiation between 311 brain tumor patients and 122 non-tumor individuals with sensitivity and specificity of 91.5% and 83.0%, respectively. The same study discriminated glioma versus meningioma, low-grade versus high-grade glioma, and groups with different organ origin of metastatic disease.

Nabers et al. [50] used an immuno-infrared-sensor in the ATR sampling mode to diagnose Alzheimer's disease (AD) in blood plasma and cerebrospinal fluid (CSF). The amide I band was specifically investigated as it reflects the overall secondary structure of amyloid-β peptides, showing a significant downshift with disease progression; the latter was attributed to increased β-sheet amyloid-β peptides. Discrimination between AD and disease control patients was achieved with accuracy 90% for CSF and 84% for plasma samples.

Rheumatoid arthritis (RA) is an autoimmune inflammatory disease with a difficult and complex diagnosis. Blood serum samples from 29 patients with RA and 40 healthy donors were collected, and ATR-FTIR spectroscopy was applied toward differentiation of the two groups. Significant differences were found in the fingerprint region as well as in a higher spectral region (3000 cm^{-1}–2800 cm^{-1}), and the two groups were classed with sensitivity and specificity of 85% and 100%, respectively [7].

Currently, a large-scale study by a diagnostics company (Glyconics Ltd.) is conducted toward diagnosis of patients with suspected respiratory disease such as chronic obstructive pulmonary disorder (COPD) in sputum samples. A preliminary diagnosis of COPD is given by spirometry, which can be insensitive and unable to distinguish between the different respiratory diseases such as COPD and asthma. Handheld ATR-FTIR systems have been used for the analysis of >500 sputum samples, showing its capacity of monitoring patients, and provide early biomarkers of acute exacerbation, which could lead to hospitalization (http://www.glyconics.com/#technology.).

6 Conclusions and Future Perspective

The field of biospectroscopy has seen tremendous progress over the last years with the focus placed extensively on disease investigation. Some of the fields that ATR-FTIR, specifically, has contributed are the development of diagnostic tools, screening of population with suspected disease, subtype classification, prediction of disease recurrence, response to treatment and personalized treatment, and much more. Despite the fact that FTIR has not yet been used for diagnosing patients

with nonspecific symptoms or for the identification of the primary origin of metastatic cancer, this possibility has been extensively discussed in a recent review [96].

Spectroscopy has been proven suitable for the differential diagnosis of various diseases with sensitivities and specificities equal (or even higher) than the ones obtained by current clinical/molecular methods. For a number of diseases, an earlier diagnosis and detection of the "warning signs" could lead to a better prognosis and immediate handling/treatment. For this reason, special attention has been given in screening of at-risk individuals before they even become symptomatic. It has been shown that this could be feasible and spectroscopy could detect changes prior to detection with conventional screening (e.g., examination of morphological changes of tissue/cells under a light microscope). One interesting example is the precancerous stages of some cancers, such as cervical or colon cancer, which may or may not progress to cancer and which spectroscopy appears to discriminate with high accuracy [37, 88, 97].

Compared to other analytical techniques which may be more sensitive, such as mass spectrometry (MS) and nuclear magnetic resonance (NMR), FTIR's ability has now been proven to generate comparable results, being able to detect and identify differential metabolites [8, 98]. The advantages of this alternative analytical method are many including high sensitivity, low cost, repeatability, and a nondestructive nature, which could render it a perfect candidate for clinical translation. In fact, it might sound surprising to someone that after all the successful applications and effort that has been put into implementation of spectroscopic techniques into the clinic, it is still not being used in routine clinical practice. The reasons for this are plenty – as already mentioned in the methodology section – including lack of standardization of techniques and sample preparation. Also, there is lack of multicenter studies with large cohort of samples (i.e., thousands), which is necessary to validate these approaches before they play a role in life-changing decisions within a clinical environment. Even though ATR is very promising, there are still several issues to be considered. As with every other analytical technique for biomarker discovery, many requirements and phases (pre-analytical, analytical, and post-analytical) need validation in independent datasets and by independent researchers before a new biomarker is approved for clinical use. In the pre-analytical phase, for example, it is important to examine whether demographic characteristics, such as age, gender, diet, or lifestyle, would affect the result. There have indeed been some examples of initially promising studies in novel biomarker discovery which were invalidated only some years after their publication [99].

A proposed scenario for clinical translation could be the use of spectroscopic methods primarily in tertiary care, with the scope that when established they will be transferred into general practice and primary care as simple and stable handheld devices, to identify patients for further examinations [53]. A recent review in vibrational spectroscopy of biological fluids states that a common mistake is to extrapolate the biomarkers' performance found in pilot studies (where a definite diagnosis of the disease has been given by gold standard methods) to the screening context [100]. Biomarker sensitivity and specificity in the screening population are expected to be much lower than in patients with confirmed disease, and thus

participants should be carefully chosen to fall into the appropriate clinical setting every time they are tested for a biomarker; this way, false-positive results would be kept at a minimum avoiding unnecessary examinations and overtreatment.

Acknowledgments We would like to thank all our collaborators over the years and all the study participants who have contributed to our research. The kind generosity of Rosemere Cancer Foundation in supporting our studies is also acknowledged; M.P. is a current recipient of one of their PhD studentships. We would also like to thank our colleagues at Lancashire Teaching Hospital NHS Trust who have selflessly facilitated many of our studies over the years. Finally, we would like to acknowledge the manufacturers for permission to copy and republish images of their instruments.

References

1. Theophilou G, Paraskevaidi M, Lima KM, Kyrgiou M, Martin-Hirsch PL, Martin FL (2015) Extracting biomarkers of commitment to cancer development: potential role of vibrational spectroscopy in systems biology. Expert Rev Mol Diagn 15(5):693–713
2. Stuart B, Infrared Spectroscopy: Fundamentals and Applications. Kirk-Othmer Encyclopedia of Chemical Technology. John Wiley & Sons, Inc. 2005; https://doi.org/10.1002/0471238961.0914061810151405.a01.pub2
3. Movasaghi Z, Rehman S, ur Rehman DI (2008) Fourier transform infrared (FTIR) spectroscopy of biological tissues. Appl Spectrosc Rev 43(2):134–179
4. Baker MJ, Trevisan J, Bassan P, Bhargava R, Butler HJ, Dorling KM et al (2014) Using Fourier transform IR spectroscopy to analyze biological materials. Nat Protoc 9(8):1771–1791
5. Mackanos MA, Contag CH (2010) Fiber-optic probes enable cancer detection with FTIR spectroscopy. Trends Biotechnol 28(6):317–323
6. Sahu R, Mordechai S (2005) Fourier transform infrared spectroscopy in cancer detection. Future Oncol 1(5):635–647
7. Lechowicz L, Chrapek M, Gaweda J, Urbaniak M, Konieczna I (2016) Use of Fourier-transform infrared spectroscopy in the diagnosis of rheumatoid arthritis: a pilot study. Mol Biol Rep 43(12):1321–1326
8. Sitole L, Steffens F, Krüger TPJ, Meyer D (2014) Mid-ATR-FTIR spectroscopic profiling of HIV/AIDS sera for novel systems diagnostics in global health. Omics J Integr Biol 18(8):513–523
9. Markus APJ, Swinkels DW, Jakobs BS, Wevers RA, Trijbels JF, Willems HL (2001) New technique for diagnosis and monitoring of alcaptonuria: quantification of homogentisic acid in urine with mid-infrared spectrometry. Anal Chim Acta 429(2):287–292
10. Khoshmanesh A, Dixon MWA, Kenny S, Tilley L, McNaughton D, Wood BR (2014) Detection and quantification of early-stage malaria parasites in laboratory infected erythrocytes by attenuated Total reflectance infrared spectroscopy and multivariate analysis. Anal Chem 86(9):4379–4386
11. Coopman R, Van de Vyver T, Kishabongo AS, Katchunga P, Van Aken EH, Cikomola J et al (2017) Glycation in human fingernail clippings using ATR-FTIR spectrometry, a new marker for the diagnosis and monitoring of diabetes mellitus. Clin Biochem 50(1–2):62–67
12. Yoshida S, Yoshida M, Yamamoto M, Takeda J (2013) Optical screening of diabetes mellitus using non-invasive Fourier-transform infrared spectroscopy technique for human lip. J Pharm Biomed Anal 76:169–176
13. Grimard V, Li C, Ramjeesingh M, Bear CE, Goormaghtigh E, Ruysschaert JM (2004) Phosphorylation-induced conformational changes of cystic fibrosis transmembrane conductance regulator monitored by attenuated Total reflection-Fourier transform IR spectroscopy and fluorescence spectroscopy. J Biol Chem 279(7):5528–5536

14. Aksoy C, Guliyev A, Kilic E, Uckan D, Severcan F (2012) Bone marrow mesenchymal stem cells in patients with beta thalassemia major: molecular analysis with attenuated total reflection-Fourier transform infrared spectroscopy study as a novel method. Stem Cells Dev 21(11):2000–2011
15. Khanmohammadi M, Garmarudi AB, Ramin M, Ghasemi K (2013) Diagnosis of renal failure by infrared spectrometric analysis of human serum samples and soft independent modeling of class analogy. Microchem J 106:67–72
16. Mulready KJ, McGoldrick D (2012) The establishment of a standard and real patient kidney stone library utilizing Fourier transform-infrared spectroscopy with a diamond ATR accessory. Urol Res 40(5):483–498
17. Graça G, Moreira AS, Correia AJV, Goodfellow BJ, Barros AS, Duarte IF et al (2013) Mid-infrared (MIR) metabolic fingerprinting of amniotic fluid: a possible avenue for early diagnosis of prenatal disorders? Anal Chim Acta 764:24–31
18. Sarroukh R, Goormaghtigh E, Ruysschaert J-M, Raussens V (2013) ATR-FTIR: a "rejuvenated" tool to investigate amyloid proteins. Biochim Biophys Acta Biomembr 1828 (10):2328–2338
19. Taylor SE, Cheung KT, Patel II, Trevisan J, Stringfellow HF, Ashton KM et al (2011) Infrared spectroscopy with multivariate analysis to interrogate endometrial tissue: a novel and objective diagnostic approach. Br J Cancer 104(5):790–797
20. Wong PTT, Lacelle S, Fung MFK, Senterman M, Mikhael NZ (1995) Characterization of exfoliated cells and tissues from human endocervix and ectocervix by FTIR and ATR/FTIR spectroscopy. Biospectroscopy 1(5):357–364
21. Gajjar K, Heppenstall LD, Pang W, Ashton KM, Trevisan J, Patel II et al (2013) Diagnostic segregation of human brain tumours using Fourier-transform infrared and/or Raman spectroscopy coupled with discriminant analysis. Anal Methods 5(1):89–102
22. Staniszewska E, Malek K, Baranska M (2014) Rapid approach to analyze biochemical variation in rat organs by ATR FTIR spectroscopy. Spectrochim Acta A Mol Biomol Spectrosc 118:981–986
23. Theophilou G, Lima KMG, Martin-Hirsch PL, Stringfellow HF, Martin FL (2016) ATR-FTIR spectroscopy coupled with chemometric analysis discriminates normal, borderline and malignant ovarian tissue: classifying subtypes of human cancer. Analyst 141(2):585–594
24. Sun X, Xu Y, Wu J, Zhang Y, Sun K (2013) Detection of lung cancer tissue by attenuated total reflection-Fourier transform infrared spectroscopy-a pilot study of 60 samples. J Surg Res 179(1):33–38
25. Kazarian SG, Chan KLA (2006) Applications of ATR-FTIR spectroscopic imaging to biomedical samples. Biochim Biophys Acta Biomembr 1758(7):858–867
26. Lima CA, Goulart VP, Côrrea L, Pereira TM, Zezell DM (2015) ATR-FTIR spectroscopy for the assessment of biochemical changes in skin due to cutaneous squamous cell carcinoma. Int J Mol Sci 16(4):6621–6630
27. Theophilou G, Lima KMG, Briggs M, Martin-Hirsch PL, Stringfellow HF, Martin FLA (2015) Biospectroscopic analysis of human prostate tissue obtained from different time periods points to a trans-generational alteration in spectral phenotype. Sci Rep 5:13465
28. Cui L, Butler HJ, Martin-Hirsch PL, Martin FL (2016) Aluminium foil as a potential substrate for ATR-FTIR, transflection FTIR or Raman spectrochemical analysis of biological specimens. Anal Methods 8(3):481–487
29. Walsh MJ, Kajdacsy-Balla A, Holton SE, Bhargava R (2012) Attenuated total reflectance Fourier-transform infrared spectroscopic imaging for breast histopathology. Vib Spectrosc 60:23–28
30. Tian P, Zhang W, Zhao H, Lei Y, Cui L, Wang W et al (2015) Intraoperative diagnosis of benign and malignant breast tissues by fourier transform infrared spectroscopy and support vector machine classification. Int J Clin Exp Med 8(1):972
31. Zohdi V, Whelan DR, Wood BR, Pearson JT, Bambery KR, Black MJ (2015) Importance of tissue preparation methods in FTIR micro-spectroscopical analysis of biological tissues:'traps for new users. PLoS One 10(2):e0116491

32. Dogan A, Lasch P, Neuschl C, Millrose MK, Alberts R, Schughart K et al (2013) ATR-FTIR spectroscopy reveals genomic loci regulating the tissue response in high fat diet fed BXD recombinant inbred mouse strains. BMC Genomics 14(1):386
33. Yao H, Shi X, Zhang Y (2014) The use of FTIR-ATR spectrometry for evaluation of surgical resection margin in colorectal cancer: a pilot study of 56 samples. Journal of. Spectroscopy 2014:4
34. Li Q-B, Sun X-J, Y-Z X, Yang L-M, Zhang Y-F, Weng S-F et al (2005) Use of Fourier-transform infrared spectroscopy to rapidly diagnose gastric endoscopic biopsies. World J Gastroenterol: WJG 11(25):3842–3845
35. Wang TD, Triadafilopoulos G, Crawford JM, Dixon LR, Bhandari T, Sahbaie P et al (2007) Detection of endogenous biomolecules in Barrett's esophagus by Fourier transform infrared spectroscopy. Proc Natl Acad Sci 104(40):15864–15869
36. Bird B, Miljkovic M, Remiszewski S, Akalin A, Kon M, Diem M (2012) Infrared spectral histopathology (SHP): a novel diagnostic tool for the accurate classification of lung cancer. Lab Investig 92(9):1358–1373
37. Gajjar K, Ahmadzai AA, Valasoulis G, Trevisan J, Founta C, Nasioutziki M et al (2014) Histology verification demonstrates that biospectroscopy analysis of cervical cytology identifies underlying disease more accurately than conventional screening: removing the confounder of discordance. PLoS One 9(1):e82416
38. Martin FL, Kelly JG, Llabjani V, Martin-Hirsch PL, Patel II, Trevisan J et al (2010) Distinguishing cell types or populations based on the computational analysis of their infrared spectra. Nat Protoc 5(11):1748–1760
39. Andrew Chan KL, Kazarian SG (2016) Attenuated total reflection Fourier-transform infrared (ATR-FTIR) imaging of tissues and live cells. Chem Soc Rev 45(7):1850–1864
40. Miljković M, Bird B, Lenau K, Mazur AI, Diem M (2013) Spectral cytopathology: new aspects of data collection, manipulation and confounding effects. Analyst 138(14):3975–3982
41. Khanmohammadi M, Ansari MA, Garmarudi AB, Hassanzadeh G, Garoosi G (2007) Cancer diagnosis by discrimination between normal and malignant human blood samples using attenuated total reflectance-Fourier transform infrared spectroscopy. Cancer Investig 25(6):397–404
42. Hoşafçı G, Klein O, Oremek G, Mäntele W (2007) Clinical chemistry without reagents? An infrared spectroscopic technique for determination of clinically relevant constituents of body fluids. Anal Bioanal Chem 387(5):1815
43. Hands JR, Dorling KM, Abel P, Ashton KM, Brodbelt A, Davis C et al (2014) Attenuated Total reflection Fourier transform infrared (ATR-FTIR) spectral discrimination of brain tumour severity from serum samples. J Biophotonics 7(3–4):189–199
44. Gajjar K, Trevisan J, Owens G, Keating PJ, Wood NJ, Stringfellow HF et al (2013) Fourier-transform infrared spectroscopy coupled with a classification machine for the analysis of blood plasma or serum: a novel diagnostic approach for ovarian cancer. Analyst 138(14):3917–3926
45. Owens GL, Gajjar K, Trevisan J, Fogarty SW, Taylor SE, Da Gama-Rose B et al (2014) Vibrational biospectroscopy coupled with multivariate analysis extracts potentially diagnostic features in blood plasma/serum of ovarian cancer patients. J Biophotonics 7(3–4):200–209
46. Lewis PD, Lewis KE, Ghosal R, Bayliss S, Lloyd AJ, Wills J et al (2010) Evaluation of FTIR spectroscopy as a diagnostic tool for lung cancer using sputum. BMC Cancer 10(1):640
47. Khaustova S, Shkurnikov M, Tonevitsky E, Artyushenko V, Tonevitsky A (2010) Noninvasive biochemical monitoring of physiological stress by Fourier transform infrared saliva spectroscopy. Analyst 135(12):3183–3192
48. Hans KM, Muller S, Sigrist MW (2012) Infrared attenuated total reflection (IR-ATR) spectroscopy for detecting drugs in human saliva. Drug Test Anal 4(6):420–429
49. Nagase Y, Yoshida S, Kamiyama K (2005) Analysis of human tear fluid by Fourier transform infrared spectroscopy. Biopolymers 79(1):18–27
50. Nabers A, Ollesch J, Schartner J, Kötting C, Genius J, Hafermann H et al (2016) Amyloid-β-secondary structure distribution in cerebrospinal fluid and blood measured by an

Immuno-infrared-sensor: a biomarker candidate for Alzheimer's disease. Anal Chem 88(5):2755–2762
51. Poste G (2011) Bring on the biomarkers. Nature 469(7329):156–157
52. Adhyam M, Gupta AKA (2012) Review on the clinical utility of PSA in cancer prostate. Indian J Surg Oncol 3(2):120–129
53. Mitchell AL, Gajjar KB, Theophilou G, Martin FL, Martin-Hirsch PL (2014) Vibrational spectroscopy of biofluids for disease screening or diagnosis: translation from the laboratory to a clinical setting. J Biophotonics 7(3–4):153–165
54. Rhodes A, Jasani B, Balaton AJ, Barnes DM, Miller KD (2000) Frequency of oestrogen and progesterone receptor positivity by immunohistochemical analysis in 7016 breast carcinomas: correlation with patient age, assay sensitivity, threshold value, and mammographic screening. J Clin Pathol 53(9):688–696
55. Humpel C (2011) Identifying and validating biomarkers for Alzheimer's disease. Trends Biotechnol 29(1):26–32
56. Swedko PJ, Clark HD, Paramsothy K, Akbari A (2003) Serum creatinine is an inadequate screening test for renal failure in elderly patients. Arch Intern Med 163(3):356–360
57. Lovergne L, Bouzy P, Untereiner V, Garnotel R, Baker MJ, Thiefin G et al (2016) Biofluid infrared spectro-diagnostics: pre-analytical considerations for clinical applications. Faraday Discuss 187(0):521–537
58. Chiappin S, Antonelli G, Gatti R, De Palo EF (2007) Saliva specimen: a new laboratory tool for diagnostic and basic investigation. Clin Chim Acta 383(1–2):30–40
59. Mitchell BL, Yasui Y, Li CI, Fitzpatrick AL, Lampe PD (2005) Impact of freeze-thaw cycles and storage time on plasma samples used in mass spectrometry based biomarker discovery projects. Cancer Informat 1:98
60. Gremlich HU, Yan B (2000) Infrared and Raman spectroscopy of biological materials, Practical Spectroscopy Series Volume 24; 2000 Sep 25, Marcel Dekker, Inc. New York, USA
61. Hands JR, Abel P, Ashton K, Dawson T, Davis C, Lea RW et al (2013) Investigating the rapid diagnosis of gliomas from serum samples using infrared spectroscopy and cytokine and angiogenesis factors. Anal Bioanal Chem 405(23):7347–7355
62. Byrne HJ, Baranska M, Puppels GJ, Stone N, Wood B, Gough KM et al (2015) Spectropathology for the next generation: quo vadis? Analyst 140(7):2066–2073
63. Deegan RD, Bakajin O, Dupont TF, Huber G, Nagel SR, Witten TA (1997) Capillary flow as the cause of ring stains from dried liquid drops. Nature 389(6653):827–829
64. Filik J, Stone N (2007) Drop coating deposition Raman spectroscopy of protein mixtures. Analyst 132(6):544–550
65. Bonnier F, Brachet G, Duong R, Sojinrin T, Respaud R, Aubrey N et al (2016) Screening the low molecular weight fraction of human serum using ATR-IR spectroscopy. J Biophotonics 9(10):1085–1097
66. Martin M, Perez-Guaita D, Andrew DW, Richards JS, Wood BR, Heraud P (2017) The effect of common anticoagulants in detection and quantification of malaria parasitemia in human red blood cells by ATR-FTIR spectroscopy. Analyst. https://doi.org/10.1039/C6AN02075E
67. Lam NYL, Rainer TH, Chiu RWK, YMD L (2004) EDTA Is A better anticoagulant than heparin or citrate for delayed blood processing for plasma DNA analysis. Clin Chem 50 (1):256–257
68. Bassan P, Lee J, Sachdeva A, Pissardini J, Dorling KM, Fletcher JS et al (2013) The inherent problem of transflection-mode infrared spectroscopic microscopy and the ramifications for biomedical single point and imaging applications. Analyst 138(1):144–157
69. Sammon C, Schultz ZD, Kazarian S, Barr H, Goodacre R, Graham D et al (2016) Spectral pathology: general discussion. Faraday Discuss 187(0):155–186
70. Trevisan J, Angelov PP, Carmichael PL, Scott AD, Martin FL (2012) Extracting biological information with computational analysis of Fourier-transform infrared (FTIR) biospectroscopy datasets: current practices to future perspectives. Analyst 137(14):3202–3215

71. Krafft C, Steiner G, Beleites C, Salzer R (2009) Disease recognition by infrared and Raman spectroscopy. J Biophotonics 2(1–2):13–28
72. Butler HJ, Ashton L, Bird B, Cinque G, Curtis K, Dorney J et al (2016) Using Raman spectroscopy to characterize biological materials. Nat Protoc 11(4):664–687
73. Glassford SE, Byrne B, Kazarian SG (2013) Recent applications of ATR FTIR spectroscopy and imaging to proteins. Biochim Biophys Acta (BBA) Proteins Proteomics 1834 (12):2849–2858
74. Ataka K, Stripp ST, Heberle J (2013) Surface-enhanced infrared absorption spectroscopy (SEIRAS) to probe monolayers of membrane proteins. Biochim Biophys Acta (BBA) Biomembranes 1828(10):2283–2293
75. JY X, Chen TW, Bao WJ, Wang K, Xia XH (2012) Label-free strategy for in-situ analysis of protein binding interaction based on attenuated Total reflection surface enhanced infrared absorption spectroscopy (ATR-SEIRAS). Langmuir 28(50):17564–17570
76. Adato R, Altug H (2013) In-situ ultra-sensitive infrared absorption spectroscopy of biomolecule interactions in real time with plasmonic nanoantennas. Nat Commun 4:2154
77. Kazarian SG, Chan KLA (2013) ATR-FTIR spectroscopic imaging: recent advances and applications to biological systems. Analyst 138(7):1940–1951
78. Mordechai S, Shufan E, Porat Katz BS, Salman A (2017) Early diagnosis of Alzheimer's disease using infrared spectroscopy of isolated blood samples followed by multivariate analyses. Analyst 142:1276
79. Walsh MJ, German MJ, Singh M, Pollock HM, Hammiche A, Kyrgiou M et al (2007) IR microspectroscopy: potential applications in cervical cancer screening. Cancer Lett 246(1–2):1–11
80. Abbasi F, Mirzadeh H, Katbab AA (2002) Bulk and surface modification of silicone rubber for biomedical applications. Polym Int 51(10):882–888
81. Tsai D-H, Davila-Morris M, DelRio FW, Guha S, Zachariah MR, Hackley VA (2011) Quantitative determination of competitive molecular adsorption on gold nanoparticles using attenuated total reflectance–Fourier transform infrared spectroscopy. Langmuir 27(15):9302–9313
82. Biazar E, Khorasani M, Daliri M (2011) Cell sheet engineering: solvent effect on nanometric grafting of poly-N-isopropylacrylamide onto polystyrene substrate under ultraviolet radiation. Int J Nanomedicine 6:295–302
83. Biazar E, Heidari M, Asefnejad A, Montazeri N (2011) The relationship between cellular adhesion and surface roughness in polystyrene modified by microwave plasma radiation. Int J Nanomedicine 6:631–639
84. Meenach SA, Vogt FG, Anderson KW, Hilt JZ, McGarry RC, Mansour HM (2013) Design, physicochemical characterization, and optimization of organic solution advanced spray-dried inhalable dipalmitoylphosphatidylcholine (DPPC) and dipalmitoylphosphatidylethanolamine poly(ethylene glycol) (DPPE-PEG) microparticles and nanoparticles for targeted respiratory nanomedicine delivery as dry powder inhalation aerosols. Int J Nanomedicine 8:275–293
85. Mudunkotuwa IA, Minshid AA, Grassian VH (2014) ATR-FTIR spectroscopy as a tool to probe surface adsorption on nanoparticles at the liquid-solid interface in environmentally and biologically relevant media. Analyst 139(5):870–881
86. Beleites C, Neugebauer U, Bocklitz T, Krafft C, Popp J (2013) Sample size planning for classification models. Anal Chim Acta 760:25–33
87. Kalmodia S, Parameswaran S, Yang W, Barrow CJ, Krishnakumar S (2015) Attenuated Total reflectance Fourier transform infrared spectroscopy: an analytical technique to understand therapeutic responses at the molecular level. Sci Rep 5:16649
88. Kelly JG, Angelov PP, Trevisan J, Vlachopoulou A, Paraskevaidis E, Martin-Hirsch PL et al (2010) Robust classification of low-grade cervical cytology following analysis with ATR-FTIR spectroscopy and subsequent application of self-learning classifier eClass. Anal Bioanal Chem 398(5):2191–2201
89. Lane R, Seo SS (2012) Attenuated Total reflectance Fourier transform infrared spectroscopy method to differentiate between normal and cancerous breast cells. J Nanosci Nanotechnol 12(9):7395–7400

90. Holton SE, Walsh MJ, Bhargava R (2011) Subcellular localization of early biochemical transformations in cancer-activated fibroblasts using infrared spectroscopic imaging. Analyst 136(14):2953–2958
91. Purandare NC, Patel II, Trevisan J, Bolger N, Kelehan R, von Bunau G et al (2013) Biospectroscopy insights into the multi-stage process of cervical cancer development: probing for spectral biomarkers in cytology to distinguish grades. Analyst 138(14):3909–3916
92. BB W, Gong YP, XH W, Chen YY, Chen FF, Jin LT et al (2015) Fourier transform infrared spectroscopy for the distinction of MCF-7 cells treated with different concentrations of 5-fluorouracil. J Transl Med 13(1):108
93. Halliwell DE, Kyrgiou M, Mitra A, Kalliala I, Paraskevaidis E, Theophilou G et al (2016) Tracking the impact of excisional cervical treatment on the cervix using biospectroscopy. Sci Rep 6:38921
94. Titus J, Filfili C, Hilliard JK, Ward JA, Unil Perera A (2014) Early detection of cell activation events by means of attenuated total reflection Fourier transform infrared spectroscopy. Appl Phys Lett 104(24):243705
95. Hands JR, Clemens G, Stables R, Ashton K, Brodbelt A, Davis C et al (2016) Brain tumour differentiation: rapid stratified serum diagnostics via attenuated total reflection Fourier-transform infrared spectroscopy. J Neuro-Oncol 127(3):463–472
96. Hughes C, Baker MJ (2016) Can mid-infrared biomedical spectroscopy of cells, fluids and tissue aid improvements in cancer survival? A patient paradigm. Analyst 141(2):467–475
97. Argov S, Ramesh J, Salman A, Sinelnikov I, Goldstein J, Guterman H et al (2002) Diagnostic potential of Fourier-transform infrared microspectroscopy and advanced computational methods in colon cancer patients. J Biomed Opt 7(2):248–254
98. Ellis DI, Goodacre R (2006) Metabolic fingerprinting in disease diagnosis: biomedical applications of infrared and Raman spectroscopy. Analyst 131(8):875–885
99. Diamandis EP (2010) Cancer biomarkers: can we turn recent failures into success? J Natl Cancer Inst 102:1462
100. Baker MJ, Hussain SR, Lovergne L, Untereiner V, Hughes C, Lukaszewski RA et al (2016) Developing and understanding biofluid vibrational spectroscopy: a critical review. Chem Soc Rev 45(7):1803–1818